WDL-TR2366
2 January 1965

THERMAL CONTROL

COMET AND CLOSE-APPROACH ASTEROID MISSION STUDY

FINAL REPORT

VOL. 8

This work was performed for the Jet Propulsion Laboratory, California Institute of Technology, sponsored by the National Aeronautics and Space Administration under Contract NAS7-100.

Prepared for

Jet Propulsion Laboratory
Pasadena, California

WDL-TR2366
2 January 1965

THERMAL CONTROL

COMET AND CLOSE-APPROACH ASTEROID MISSION STUDY

FINAL REPORT

VOLUME 8

Contract JPL 950870

Prepared by

PHILCO CORPORATION
A Subsidiary of Ford Motor Company
WDL Division
Palo Alto, California

Prepared for

Jet Propulsion Laboratory
Pasadena, California

FOREWORD

This document is the final report of work performed on Thermal Control by the WDL Division of the Philco Corporation during the Comet and Close-Approach Asteroid Mission Study for the Jet Propulsion Laboratory under Contract JPL 950870. The report covers work performed during the period 2 July 1964 to 2 January 1965.

ACKNOWLEDGMENT

This volume was prepared by Joel Kayne, Michael Cobb and Don Newell.

SUMMARY

The basic approach to the Comet Probe thermal design is to minimize the effect of the external environment and to achieve equipment temperature control by judiciously using thermal control surfaces in conjunction with internal heat generation. The effect of the large variation in solar heat load is reduced by orienting the spacecraft to the sun and utilizing a heat shield on the side that always "sees" the sun. The desired heat shield performance is obtained with multiple-foil insulation if heat leaks through supports and edges are minimized. The effect of cold black space is reduced by utilizing either multiple-foil insulation and/or coatings with low infrared emittance on other than temperature controlled surfaces. This prevents sub-cooling of the equipment compartment and also directs the heat flow to surface is that can be controlled either by passive or active techniques.

The passive technique of temperature control, utilizing surface optical properties is the preferred method due to its inherent reliability and minimum weight penalty, and is used as much as possible. However, heat dissipations vary in magnitude and location due to the turning on and off of components and a single coating may not be capable of maintaining the desired temperature. This is a particular problem with the battery where fine temperature control is required and large heat loads are generated for short periods of time. Therefore, an active temperature control device must be used. However, the number of active units can be minimized by careful location of components and by maintaining their composite heat dissipation fairly constant.

In areas where surfaces "see" the sun, the design attempts to use coatings whose optical properties of solar absorptance and infrared emittance are equal. This is intended to eliminate the problems in present-day solar simulation techniques in their ability to match the solar spectrum, energy and columnation. This allows the spacecraft to be thoroughly assessed by

ground testing with confidence in results. The coatings and material study was directed toward obtaining coatings that have properties over the complete spectrum of absorptance and emittance and also others that are flat reflectors or absorbers across the complete wave length band. A number of coatings based upon five $\alpha s/\epsilon$ requirements have been obtained that will maintain their properties when subjected to the Comet Probe launch and flight environment.

During the study, parametric curves have been generated which, given the surface properties for a sphere, cube and cylinder, determine the temperature range from 1 to 2 A.U. as a function of internal heat dissipation and dimensions. These curveswere used to predict the temperature range for the magnetrometer and ionization chamber. In addition, preliminary calculations have been conducted to determine the surface characteristics and design of the isotopic power supply, DC-DC converter, heat shield, high-gain antenna and scan platform.

The effect of spacecraft misalignment to the sun due to midcourse corrections has been investigated and found to be no problem with regard to the internal equipment. However, temperatures of low emitting surfaces may exceed their limits depending upon the solar distance when the maneuvers occur. This problem requires further investigation.

Although a major portion of the Mariner-C thermal design and technology is directly applicable to Comet Probe designs, particularly in the active temperature control areas, three areas require further study: (1) study of methods of mounting multiple-foil insulation with minimum thermal shorting that will withstand the acceleration and vibration environment imposed during boost, (2) testing of certain coatings for the total amount of equivalent sun hours that occur in Comet Probe missions, (3) evaluation of possible methods of obtaining structural joints that change thermal characteristics after launch.

TABLE OF CONTENTS

LIST OF ILLUSTRATIONS

LIST OF TABLES

SECTION 1
OBJECTIVES AND REQUIREMENTS

1.1 DESIGN REQUIREMENTS

The objective of the thermal control subsystem is to maintain the spacecraft, its components, and the scientific instruments within their operating limits during all phases of the mission. The major requirements imposed on the subsystem are the following:

1. Maintain the temperature limits for critical and less critical components, as given in Table 1-1.
2. Operate for at least one year over heliocentric distances from 1.0 to 2.0 A.U.
3. Function properly over a wide range of heat source location and electrical duty cycles, as shown in Figure 1-1.
4. Be capable of being ground tested with a high level of confidence in test results.
5. Operate with high reliability with a minimum weight penalty.

The following sections analyze the temperature control subsystem tradeoffs for two spacecraft power configurations, discuss the investigations of problem areas, and outline unresolved problems.

Table 1-1 Comet Probe Equipment Characteristics

Item	Weight (lbs.)	Heat Dissipation (w)	Temperature Limits (°F)	Remarks
A. Scientific Instruments				
1. Helium Vapor Electronics	4.8	7.0	0 to 150	
Magnetometer Sensor	1.3		-65 to 130	Located away from equipment bay
2. Piezoelectric Dust Detector	2.3	0.215	-40 to 160	
3. Electrostatic Plasma Probe	7.0	3.5	14 to 175	On instrument bay
4. Integrating Ionization Chamber	2.6	0.5	-22 to 158	
5. Planar - Trap Electron Detector	8.0	2.0	--	
6. Lyman - Alpha Photometer	1.5	1.5	0 to 122	
7. Bistatic Radar Receiver	10.0	5.0	-40 to 212	
8. Slow-Scan T.V.	11.7	9.0	0 to 120	Scan Platform
9. IR Photo-Multiplier Radiometer	3.0	3.0	0 to 120	Scan Platform
10. IR Spectrometer	29.0	4.0	0 to 120	Shade from sun
11. UV Spectrometer	22.0	12.0	0 to 120	Shade from sun Scan Platform
12. UV Photometer	6.0	6.0	0 to 120	Shade from sun*
13. Ion Mass Spectrometer	8.0	8.0	--	
B. Communication				
1. Transponder	11.0	28.0	14 to 167	Equipment Bay
2. 10-Watt Power Amplifier	10.0	40.0	30 to 120	Equipment Bay
3. 25-Watt Power Amplifier	15.0	75 to 100	30 to 120	Equipment Bay

* Two may be on scan platform

Table 1-1 Comet Probe Equipment Characteristics (Continued)

Item	Weight (lbs.)	Heat Dissipation (w)	Temperature Limits (°F)	Remarks
B. Communication (Continued)				
4. Ranging Module	6.0	3.0	14 to 167	Equipment Bay
5. Command Decoder	4.0	3.0	14 to 167	Equipment Bay
6. Command Detector	4.0	2.0	14 to 167	Equipment Bay
7. Tape Recorder	8.0	7.0	0 to 120	Equipment Bay
8. Data Encoding and Processing	25.0	15.0	14 to 167	Equipment Bay
9. High-Gain Antenna	7 - 10	--	150 maximum	Minimize Temperature Gradient
10. Preamplifier	1.0	0.05	14 to 167	Equipment Bay
C. Guidance and Control				
1. Sun Sensor	0.4	--	-20 to 185	See sun continuously
2. Electronic Amplifier, Harness, Torque Logic	9.5	6.0	-20 to 65	
3. Gas Tank, Regulator, 4.2 Manifold, Plumbing and Gas	28.0	3(maximum) 0.003 (cont.)	-30 to 250	
4. Solar Vanes	3.0	--	-30 to 250	
5. Star Tracker	5.5	8.0	-40 to 150	Maintain < 1° gradient across unit, view stars
6. Radio Null System (Electronics)	5.0	6.0	0 to 150	
7. Autopilot, 4 Clocks, Decoder, Hardness, Structure	18.8	8.0	0 to 150	
8. (3) Gyros, Heaters, Torque Ampere Resolvers, and Wheel Power	11.0	54 Operating 30(Heater maint)	113 ± 5.4	Maintain minimum temperature variation
9. Post-Ignition Propulsion	100	--	35 to 125	

Table 1-1 Comet Probe Equipment Characteristics (Continued)

Item	Weight (lbs.)	Heat Dissipation (w)	Temperature Limits (°F)	Remarks
D. Power				
1. DC-DC Converter	8.0	30.0	0 to 150	
2. Battery (Silver-Zinc)		1.5 to 30	50 to 120	

Fig. 1-1 Power Profile vs Mission Time

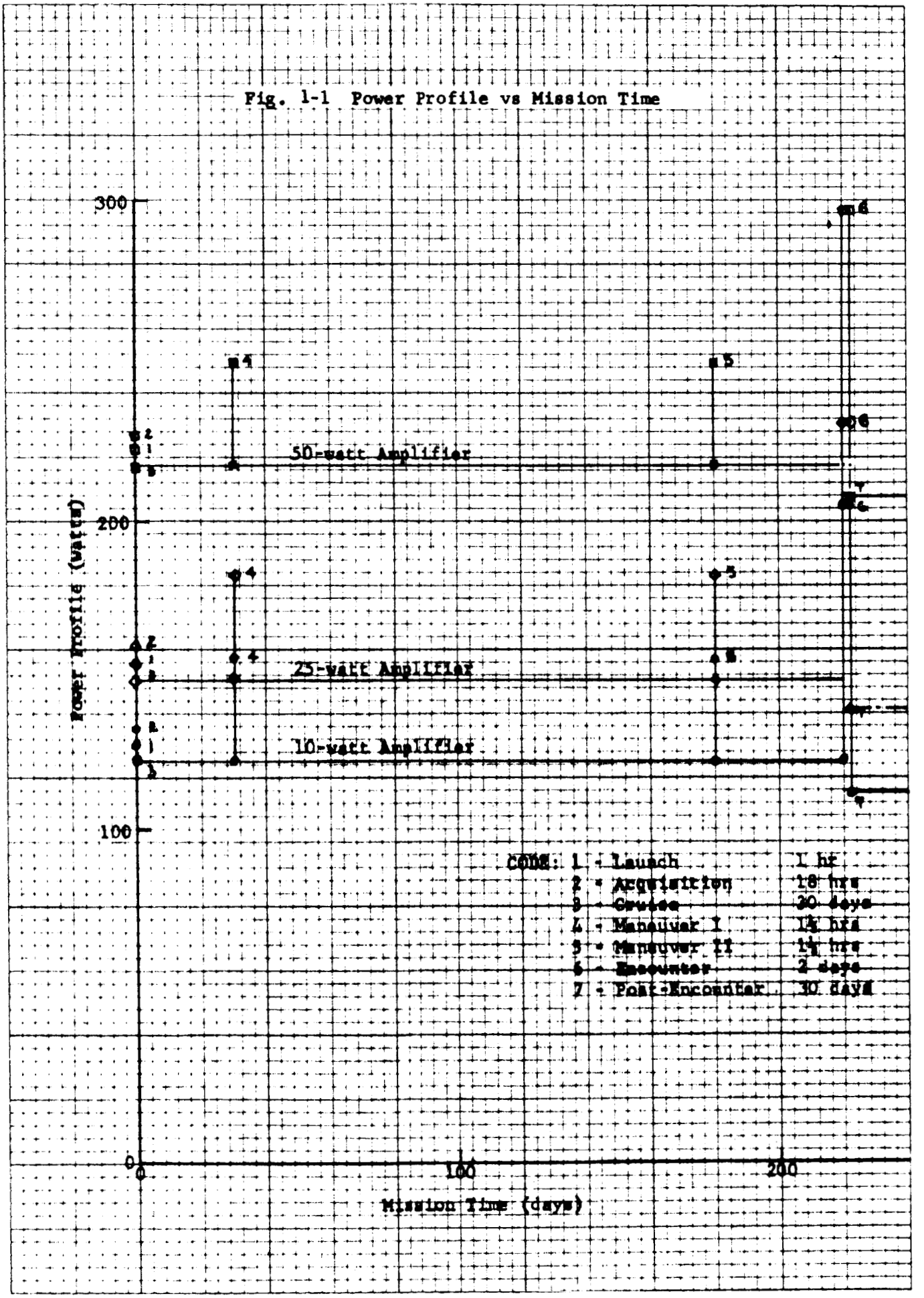

SECTION 2
THERMAL CONTROL SUBSYSTEM

2.1 THERMAL SHIELD

Since the distance between the spacecraft and sun changes for the missions under investigation, the variation of solar heating, as indicated in Figure 2-2, imposes the most severe condition on the temperature control subsystem. This condition is minimized by orienting a spacecraft z axis at the sun and by applying a heat shield on the side that "sees" the sun. Instruments and components that require a closely controlled environment are located in a compartment protected by the shield.

Two spacecraft configurations have evolved from shroud constraints and the choices of power subsystems, i.e., solar panels and radioisotopes. The thermal control subsystem for each is illustrated in Figures 2-3 and 2-4. There is basically little difference between configurations with regard to thermal control design. It can be noted in both designs that surfaces that "see" the sun have, in most cases, coatings where the solar absorptance is equal to the emittance. This is a major constraint imposed on the thermal design to insure a design that can be thoroughly assessed by ground tests. This is directed at eliminating the problems associated with present-day solar simulation capabilities as compared with actual conditions.

2.2 INSULATION

Each design has a solar shield that combines the shading of the antenna with multiple-foil insulation. The isotopic configuration has an additional shield to reduce the energy interchange between isotope and equipment compartment. It also allows a low emissive coating on the insulation external surface, thereby increasing the protective capability of the insulation. The adequacy of these designs in preventing heat leakage into or out of the spacecraft is illustrated in Figure 2-5 and 2-6.

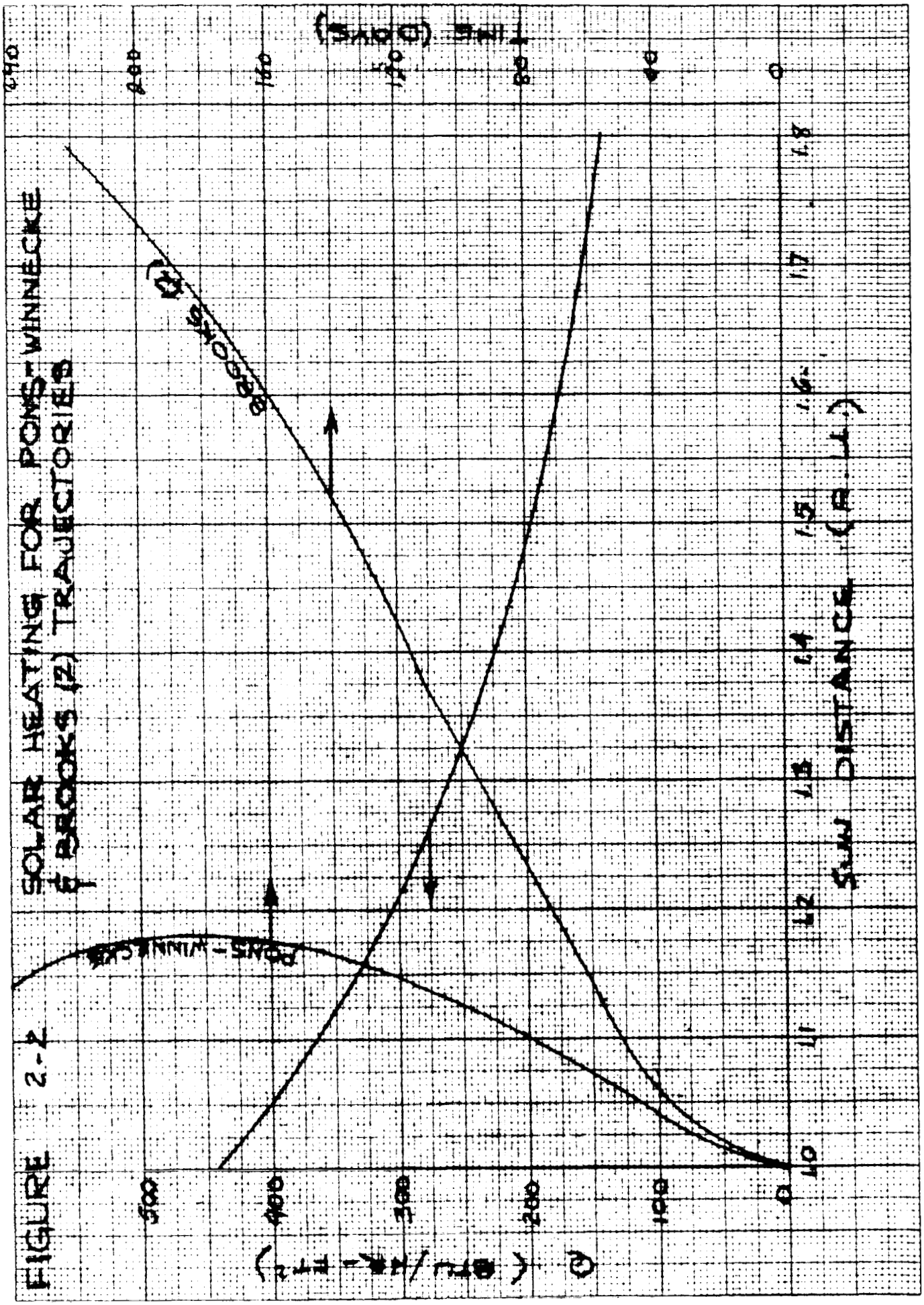
SOLAR HEATING FOR PONS-WINNECKE & BROOKS (2) TRAJECTORIES
SUN DISTANCE (R.U.)
PONS - WINNECKE
BROOKS (2)

FIGURE 2-2

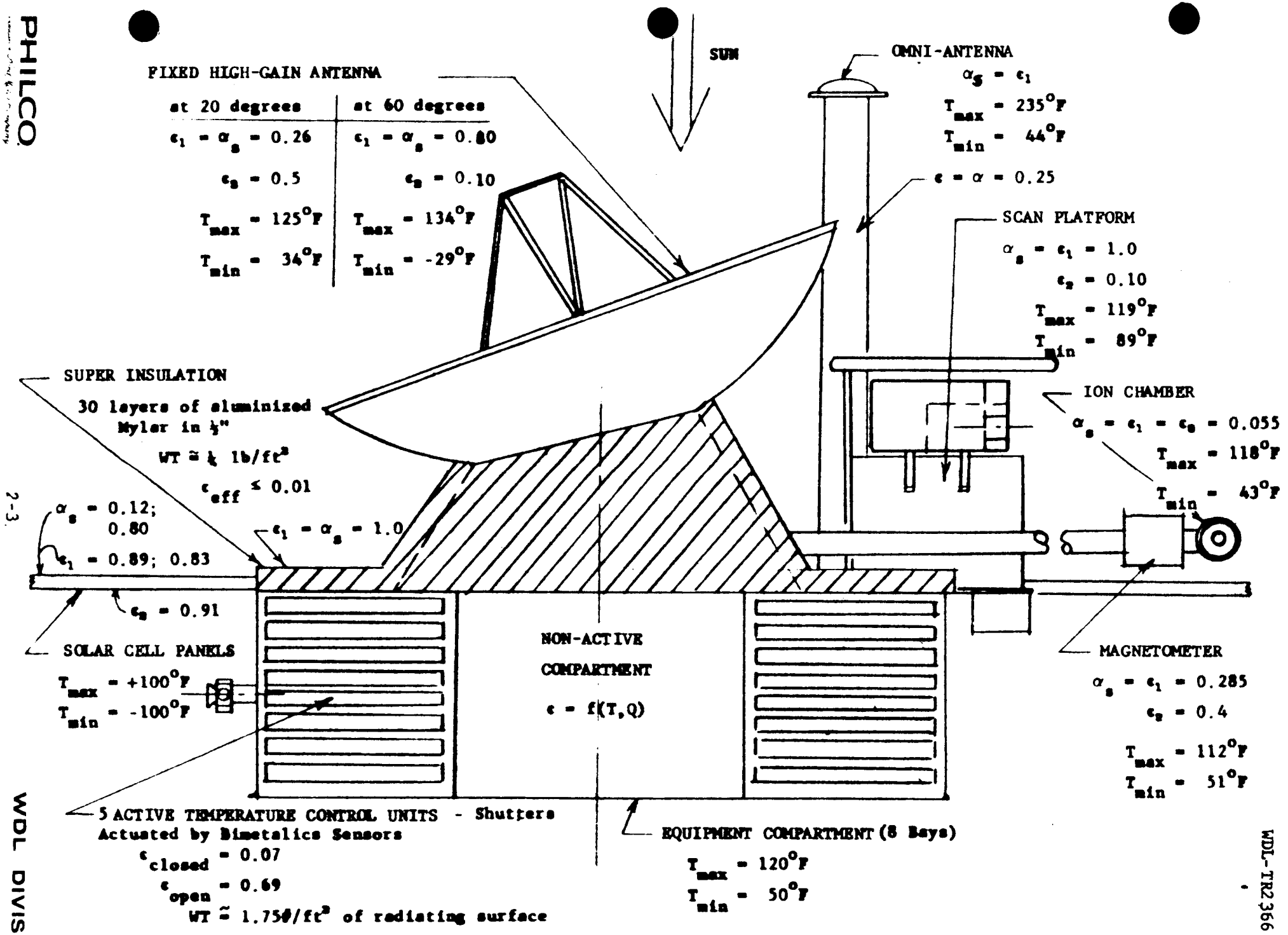

Fig. 2-3 Solar Panel Vehicle Thermal Design

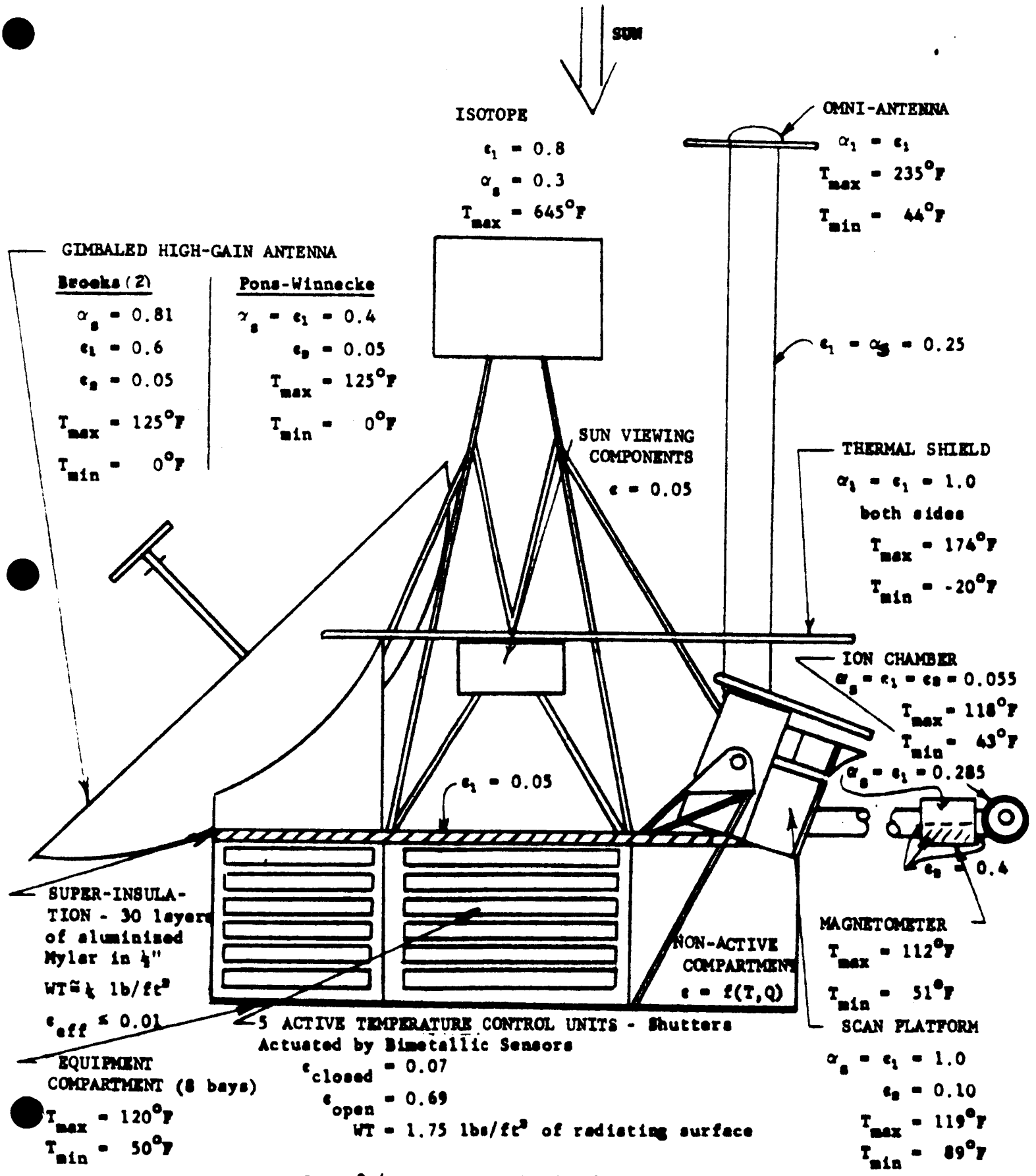

Fig. 2-4 Isotope Vehicle Thermal Design

Fig. 2-5 Comet Probe Insulation Effectiveness (Solar Panel Design)

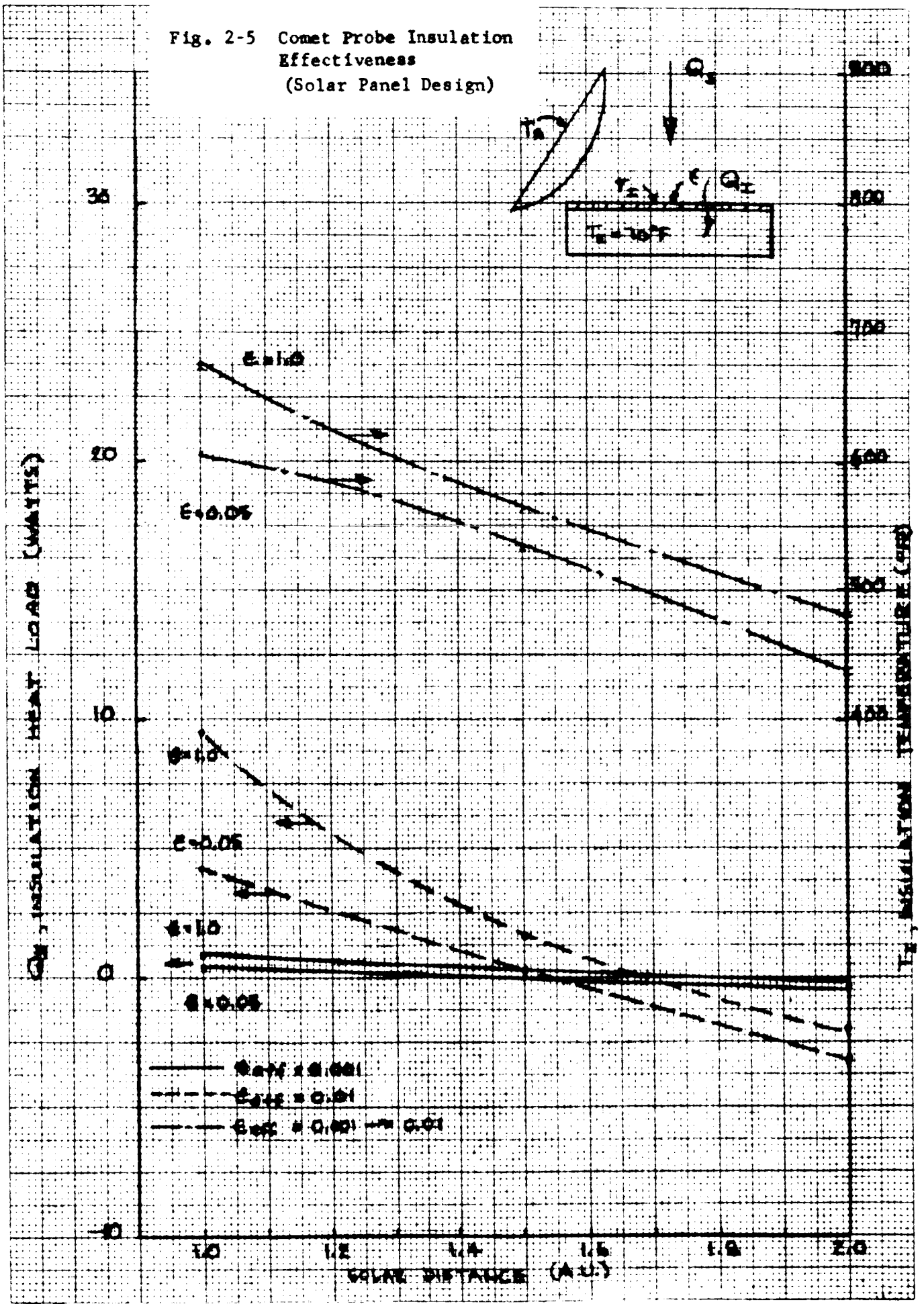

Fig. 2-6 Comet Probe Insulation Effectiveness with One Thermal Shield (Isotope Design)

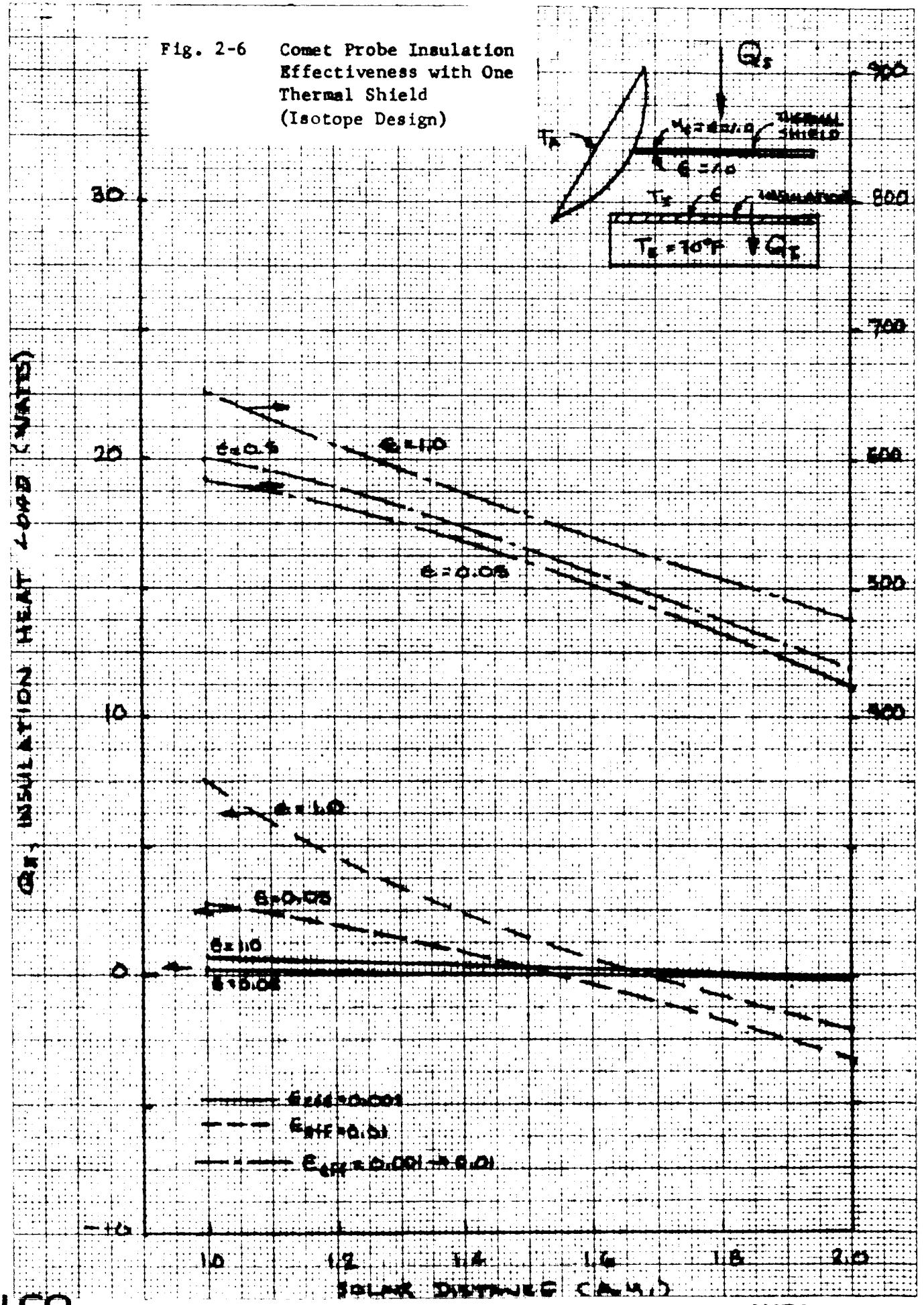

Insulation test results published by National Research Corporation [1959], General Electric Casagrande, [1962], and Philco WDL [1963] indicate that an overall effective emissivity of 0.01 is very conservative, particularly where the fasterner and edge area is much less than the covered area. Assuming this effective emissivity, an equipment compartment temperature of 70°F (530°R) and an external insulation emissivity (aborptivity) of unity the heat input at 1 A.U. is +9.6 watts for the solar panel design. This results in a heat leak at 2 A.U. of only -1.9 watts which is well within the allowable limit of -30 watts.

The isotopic design has a heat input into the spacecraft from the sun of only +3.0 watts, assuming the shield has an absorptivity (emissivity) of 1.0 and the insulation external emissivity is 0.05. Again the effective emissivity is taken at 0.01. The insulation design recommended for the heat shield consists of 30 layers of crinkled aluminized mylar stacked to a height of 1/2 inch. The external surface material is a heat-conductor to dissipate the heat absorbed from the sun by the shield and/or antenna, over the complete insulation area and, thereby, prevent local hot spots. This material, perhaps aluminum for its low emissive characteristic, could also support a coating if required. The insulation is attached with a minimum of fasteners, preferably ceramic-type bolts, and properly overlapped to prevent edge losses. The total shield weight for the solar panel design is less than 4 lbs. while the isotpic design is less than 8 lbs.

2.3 ACTIVE CONTROL

With the effect of the external environment negated, equipment temperature control is then maintained by judiciously using thermal control surfaces in conjunction with internal heat generation. The radiating surface area of the equipment compartment on the remaining sides of the spacecraft that "see" only cold space in both designs are sufficient to dissipate the expected peak load of 375 watts. Due to the cycling of equipment during the mission, active temperature control in the form of moveable shutters is used. The design employed on the Mariner-C has sufficient performance to be applicable here. The number of active units can be minimized by carefully locating

the components. A compartment whose heat dissipation during the mission is fairly constant due to the cycling on of units when others are off can utilize the more reliable and less weighty passive technique for control. Active control can not be totally eliminated but can be optimized as the equipment and their heat-dissipation cycles become better known during a detailed design. The present design utilizes 5 active units at a total weight of less than 21 lbs. based on a unit weight of 1.75 lbs/ft^2 of radiating area.

The equipment is mounted directly to the radiating surface to minimize internal heat conduction and thereby, increase the efficiency of the radiating surface. This results in an integrated temperature control system and equipment package.

All surfaces not used for temperature control are covered either with super-insulation or a low-emissive coating, depending upon the ratio of edge and fastener area, to total areas, complexity of design and total performance required. This is to prevent sub-cooling of the equipment and to minimize energy interchange with solar panels and extended booms. Assuming an effective emissivity of 0.01, the total heat leak is 9.1 watts. The weight of this insulation is approximately 6.9 lbs. This brings the total weight of the thermal control subsystem to about 32 lbs. for the solar panel design and 36 lbs. for the isotopic design.

2.4 EXTERNAL EQUIPMENT

Serious thermal design problems associated with the variation in solar heating other than the main equipment compartment are spacecraft appendages, such as solar panels, the high-gain antenna and scientific instruments mounted directly on the spacecraft and/or booms. Steady-state temperature control of the solar panels in conjunctoin with the power design is discussed in detail in Volume 7 on power. However, panel temperatures can fall well below -100°F during a manuever should the panels become oriented edgewise to the sun. The severity of this problem can be noted in Figure 2-7 where the temperatures can drop as low as -224°F within two hours, assuming

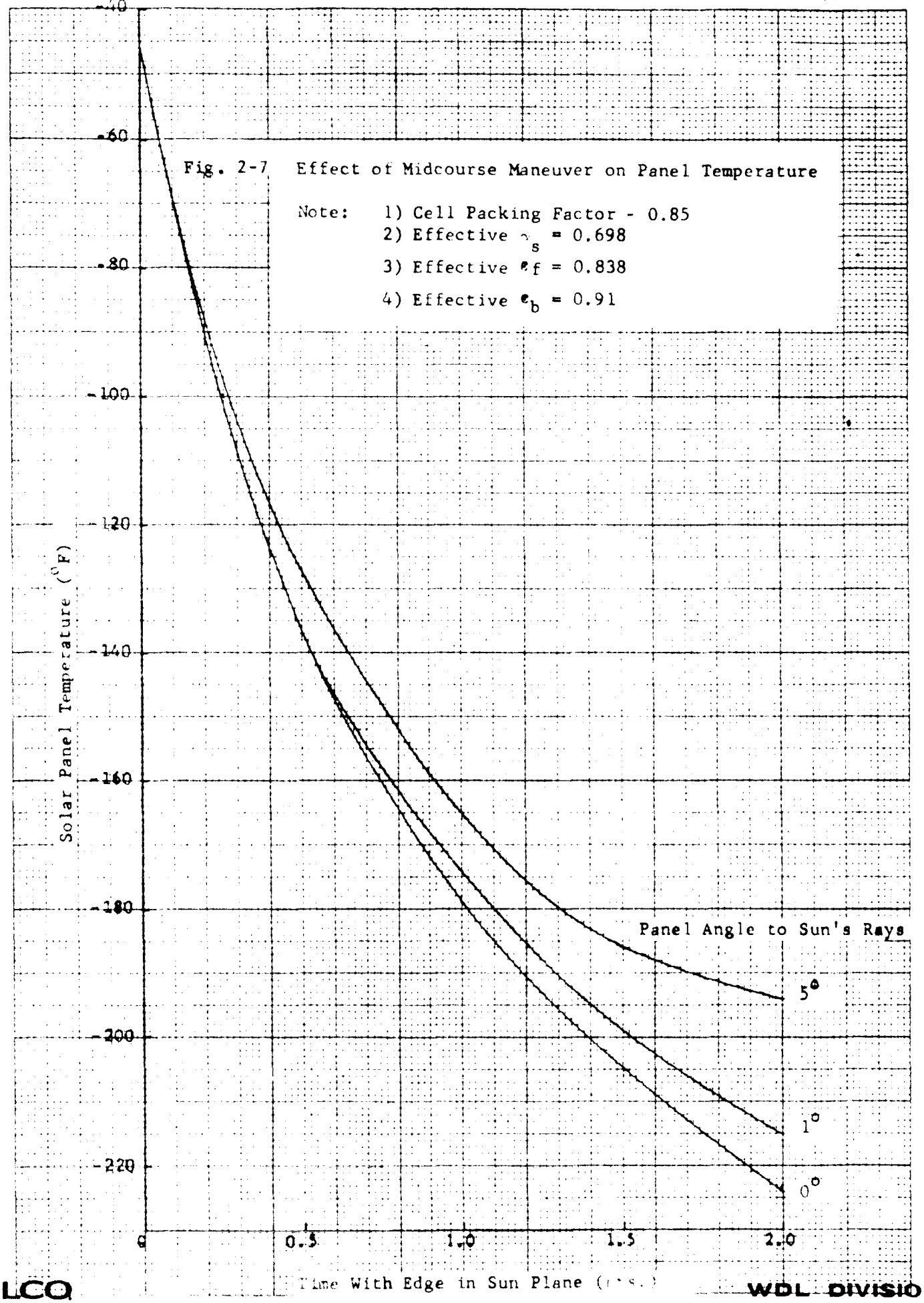

Fig. 2-7 Effect of Midcourse Maneuver on Panel Temperature

Note:
1) Cell Packing Factor - 0.85
2) Effective α_s = 0.698
3) Effective ϵ_f = 0.838
4) Effective ϵ_b = 0.91

a manuever occurs 30 days from a Brooks (2) encounter. This imposes a severe condition on the solar cell adhesive which is normally limited to a minimum temperature of -160°F. Careful consideration of panel orientation during manuevers and the limits of solar cell design must be included in any future investigations.

The temperature will range from +100° to -100°F between 1 and 2 A.U. The low temperature at 2 A.U. may impose a severe heat leak on the equipment compartment. To reduce the problem, a high thermal resistive joint is needed. The joint must also have sufficient structural integrity to support the solar panels during the boost and deployment phases. Although the two requirements are normally incompatible because a strong structural joint is inherently a good thermal conducting joint, there are a number of possible methods to achieve the desired joint characteristics.

One of these possibilities is the use of an isotope-impregnated material that would expand or vaporize due to the heat added by the isotope decay. There are some isotopes that have an increasing heat generation with time, e.g., U-232, which can be used to reach a threshold some time during the mission and, thereby, reduce the thermal continuity of the joint. This technique suggests that further exploration should be conducted.

Two possible high-gain antenna mounting techniques have been investigated: (1) a body-fixed antenna oriented to 60° off the spacecraft-sun axis; and (2) a gimbaled antenna whose axis always points toward the earth. A temperature range of -30° to +135°F can be maintained on the fixed orientation while a range from 0° to 125°F is achievable on a movable antenna. In both cases, this temperature control can be achieved by proper utilization of optical characteristics on the inside and outside surfaces. These characteristics are available in existing coatings.

In addition, three externally mounted scientific units have been examined to determine the surface optical characteristics required for temperature control. The units are the magnetometer, ion chamber, and the scan

platform which supports a UV spectro photometer, IR radiometer or UV photometers, and a slow-scan television. Parametric curves have been generated for three different shapes, viz., spherical, cylindrical and cubic, to obtain the temperature at the two extreme solar distances of 1 and 2 A.U. as a function of surface optical properties, internal heat generation and geometry. These curves indicate that a temperature range of 51 to 112°F can be obtained for the magnetometer with a solar absorptance (emittance) of 0.285 and an emissivity of 0.4 on the surfaces not having solar impingement. Further, the ion chamber can be held between 43° and 118°F with surface properties all equal to 0.055. The emissivity of the portion of the surface viewing the sun is assumed to be equal to the solar absorptance as previously discussed.

The scan platform does not fall in the same category as these instruments. Analysis indicates that fine temperature control can be obtained by utilizing a heat shield and by turning the unit on at a pre-arranged time during the flight. The maximum temperature at 1 A.U. with the units off is 119°F while the coldest with the units off at 2 A.U. is -51°F. The latter value can be raised to a respectable 89°F if the units are turned on approximately 60 days prior to recording data.

2.5 MIDCOURSE MANEUVERS

The effect of midcourse maneuvers on temperature rise rate in the equipment compartment has been evaluated assuming the following conditions:

a. Maximum misalignment of 90° from the sun-spacecraft axis.

b. Equipment compartment taken as lump mass weighing 450 lbs. and at an initial temperature of 70°F.

c. Active control shutters full open, which results in an effective emissivity of 0.69 over 12 ft^2 while the rest of the external surface is covered with super-insulation.

d. Internal heat generation at 300 watts.

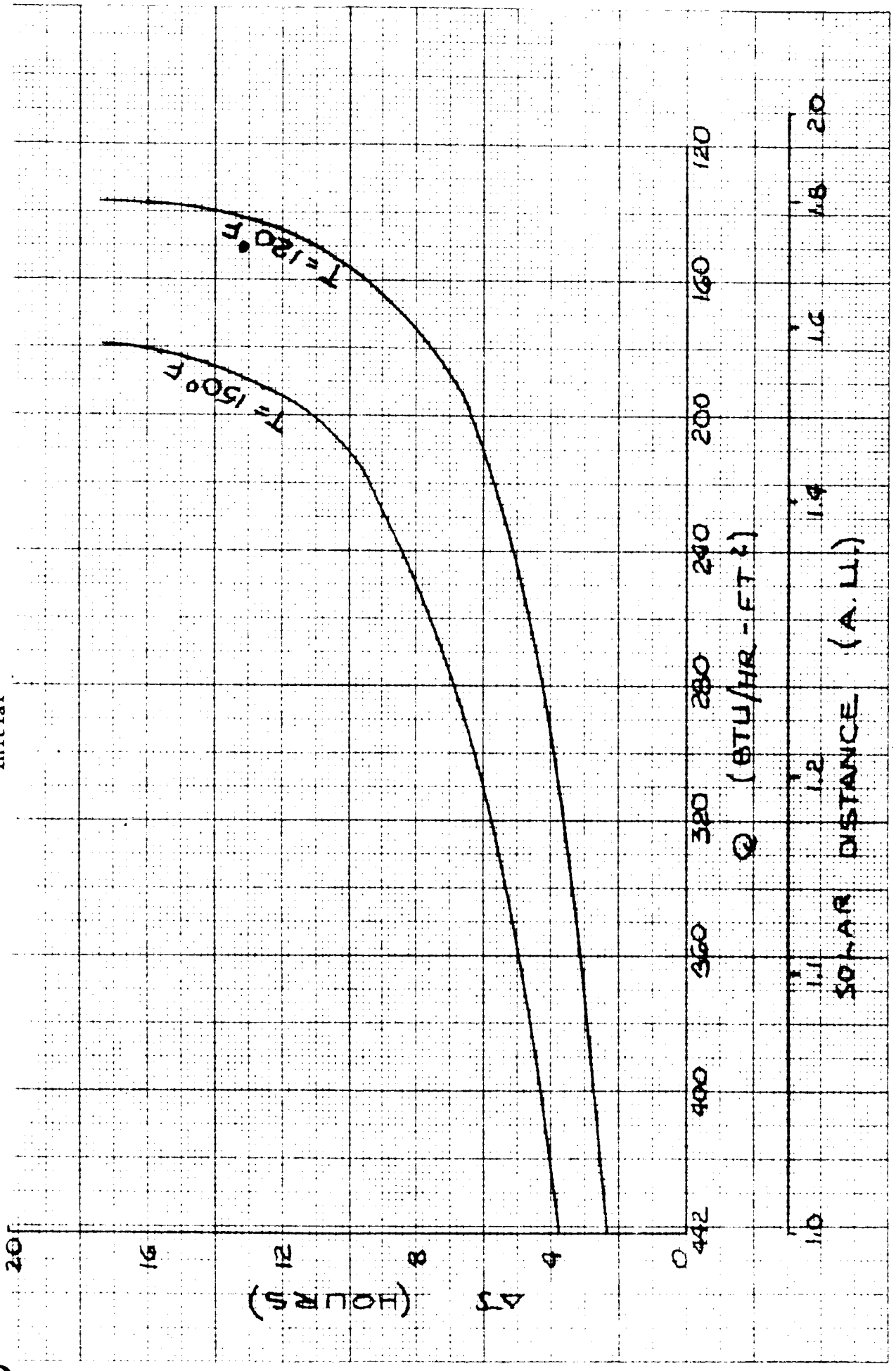

Fig. 2-8 Time to Reach 120°F and 150°F with 90° Misalignment to Sun Axis ($T_{initial}$ = 70°F)

The time to reach critical equipment temperatures of 120° and 150°F are presented in Figure 2-8 as a function of distance from sun and solar heat flux. The presently scheduled midcourse maneuvers cause a maximum misalignment of 2 hours duration which is well within the times indicated in the figure.

SECTION 3
EXTERNALLY MOUNTED EQUIPMENT

3.1 HIGH-GAIN ANTENNA

Specific analyses have been completed on the following externally mounted equipment:

a. Body-fixed and rotating high-gain antenna
b. Radioisotopic power supply and DC-DC converter
c. Boom-mounted magnetometer and ion chamber
d. Scan platform.

The high-gain antenna is assumed to be 4-foot diameter, parabolic face, and so located on the spacecraft as to have continuous solar heating during a typical mission. The major thermal problems associated with this type of antenna include, distortion in signal due to temperature gradients across the antenna, the concentration of solar energy on the feed horn, and the heat leakage with its subsequent effect on internal temperature control.

The aim of this preliminary analysis is to determine the surface characteristics that maintain the antenna temperature profile close to internal temperatures during the complete flight. This reduces the heat leakage effect and also minimizes the distortions that are created by a large gradient between antenna and support structure. The distortion due to temperature variations in this antenna has not been solved during this study because the antenna design is not totally defined and the analysis is complex and lengthy. The concentration problem is negated by utilizing a relatively high solar absorbing and diffuse coating on the inside surface and the fact that the antenna axis is not in line with the sun.

The desired surface characteristics have been determined for two antenna system designs. The first allows the antenna to rotate its axis

toward the earth. The second is a body-fixed antenna set at a pre-determined angle from the spacecraft-sun axis. This angle can range from 20° to 60°. In all cases analysed, the antenna is assumed to be an isothermal structure and the time rate of charge of the heat flux upon the antenna is slow enough to insure that the antenna is always in thermal equilibrium with its environment.

3.1.1 Rotating Antenna

A trajectory solar flux program has been used to determine the solar flux incident upon the rotating antenna. This program evaluates the solar flux incident upon a convex polyhedron with a maximum of 20 sides given as inputs the unit normal for each side, the time points at which the evaluation is to be made, and the sun-spacecraft range and earth-spacecraft-sun angle at that time. Each quadrant of the antenna surface is divided into twenty parabolic trapezoids while the interior surface of the antenna presents the appearance of a disk being rotated on an axis perpendicular to the antenna-sun line and to the ecliptic plane. Reradiation due to internal reflections of the incident flux are neglected.

The temperatures for spacecraft trajectures to Brooks (2) and Pons-Winnecke are presented in Figures 3-1 and 3-2 for two α_s/ϵ ratios of 1.0 and 2.0. The emissivity here is the sum of the inside and outside emissivities. To achieve a temperature range of 0 to 125°F (460 to 385°F), and α_s/ϵ ratio of 1.5 is indicated for the Brooks (2) mission while a ratio of 1.0 is suggested for the Pons-Winnecke Mission. The ratio of 1.5 cannot be obtained with the requirement that the emissivity be equal to the absorptivity on the irradiated surface. Therefore, a coating whose α_s/ϵ_1 ratio is 1.35 is required, where ϵ_1 is the emissivity of the irradiated surface. This value is based upon the internal surface "seeing" itself by a factor of 12.5%. On the other hand, an α_s/ϵ ratio of 1.0 is achievable within the constraint by having the ratio of internal emissivity to external emissivity equal to 8.0. A typical design consists of polished aluminum with an emissivity of 0.10 on the external surface and a green paint, developed by JPL for the Mariner-C antenna, having the flat absorber characteristics of $\alpha_s = \epsilon_s = 0.8$ for the internal surface.

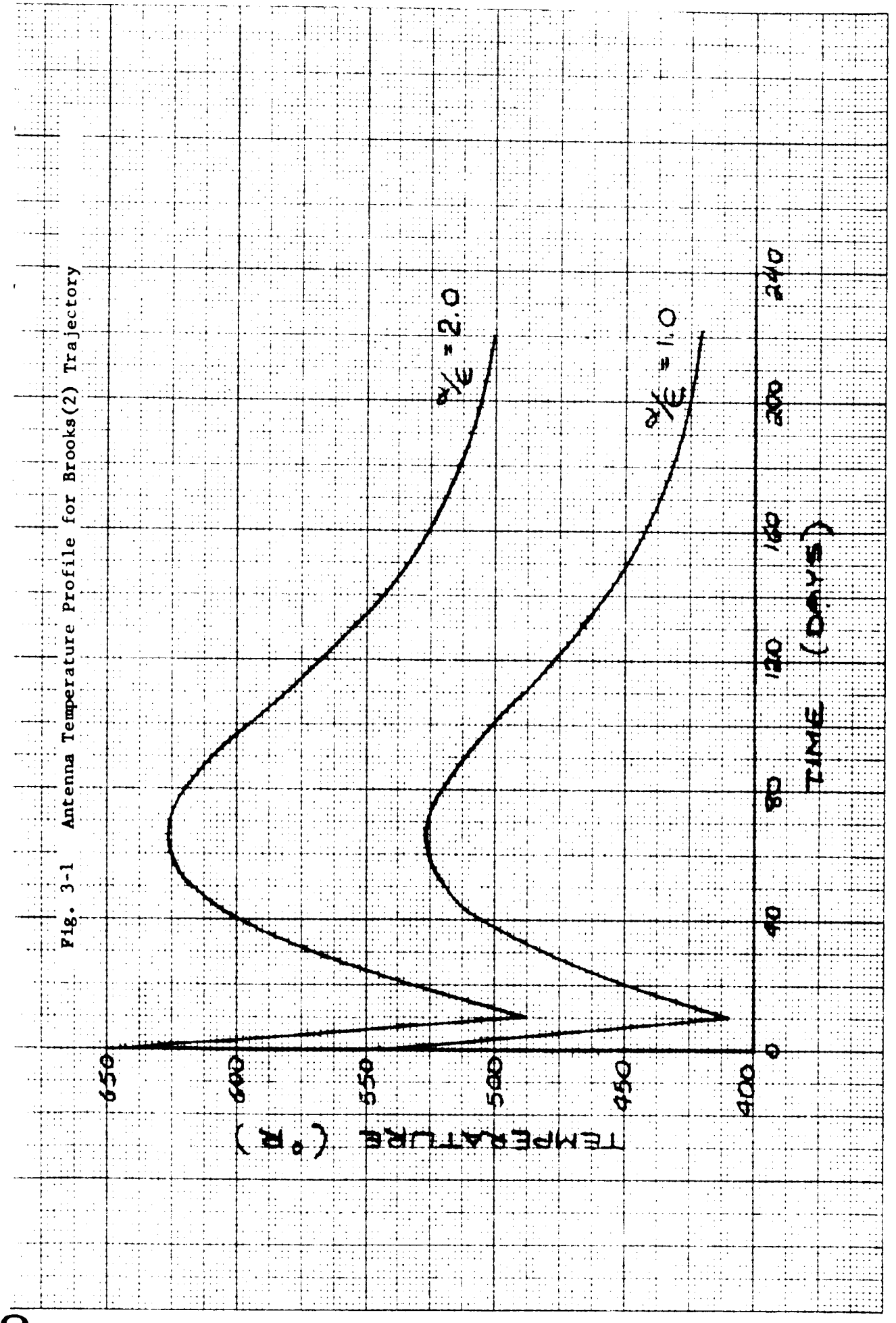

Fig. 3-1 Antenna Temperature Profile for Brooks(2) Trajectory

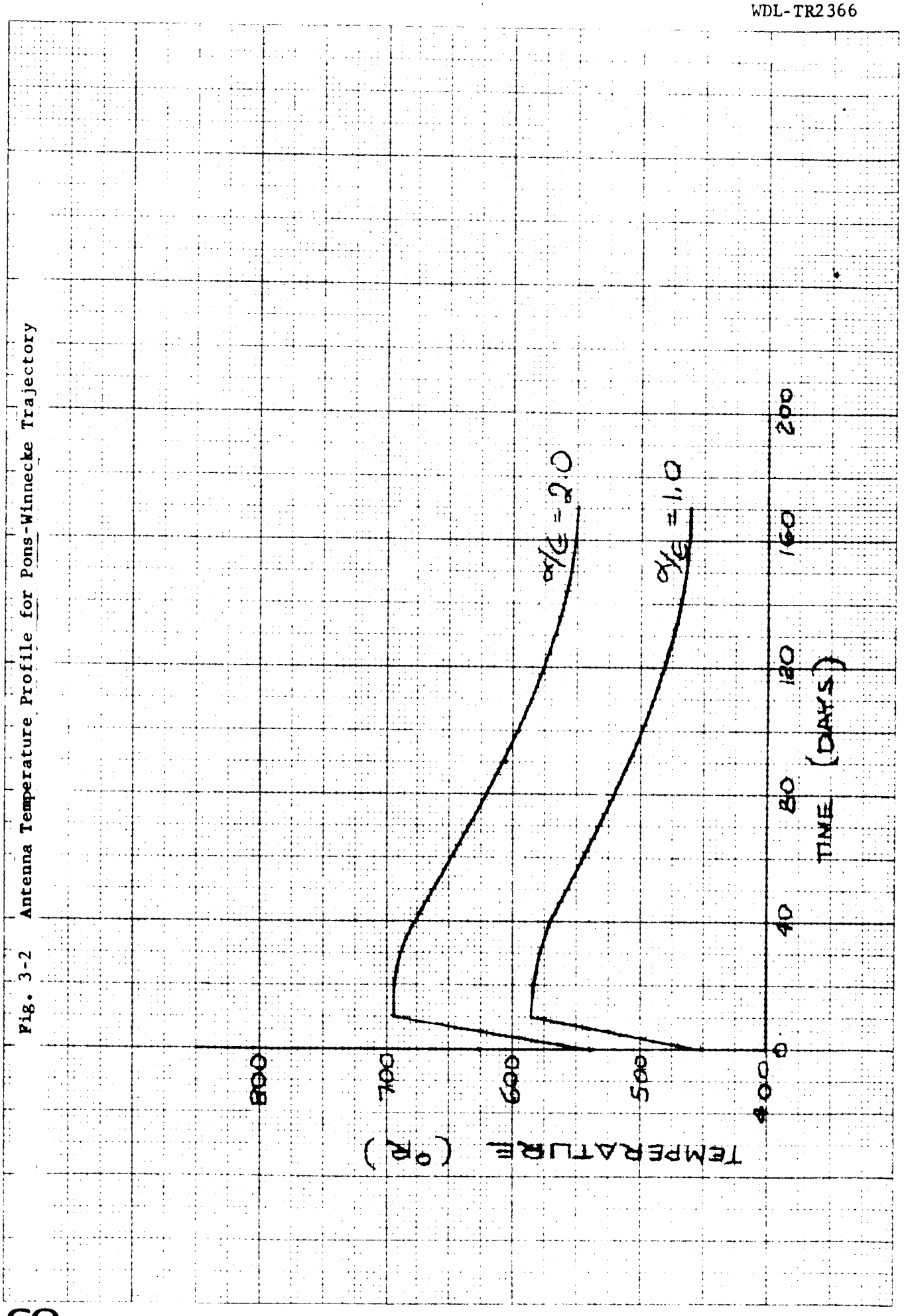

Fig. 3-2 Antenna Temperature Profile for Pons-Winnecke Trajectory

3.1.2 Fixed Antenna

The temperature of the fixed antenna has been determined from the following equation.

$$T = \left[\frac{\alpha_s \frac{Q_s}{r^2} A_p/A_1 + \sigma F_{a_{a-v}} \epsilon_2 T_v^4}{\left[\left(1-F_{a_{v-v}}\right) \epsilon_1 + \epsilon_2\right] \sigma} \right]^{\frac{1}{4}} \qquad (3\text{-}1)$$

where

$\alpha_s = \epsilon_1$ = concave-surface solar absorptivity and emissivity

Q_s = solar heat flux at 1 A.U. = 442 Btu/hr. ft^2

r = solar distance (A.U.)

A_p = projected area = $\pi(4) \cos \theta (ft^2)$

A_1 = half the total surface area = 14.2 ft^2

θ = angle between vehicle-sun axis and feed horn axis (deg.)

σ = Stefan-Boltzman constant = 0.1713×10^{-8} Btu/hr. ft^2 $(^\circ R)^4$

$F_{a_{a-v}}$ = view factor between antenna and vehicle = 0.75

ϵ_2 = emissivity of convex surface

T_v = vehicle temperature = $530^\circ F$

$F_{a_{v-v}}$ = view factor of antenna concave surface to itself = 0.125

For a 20° orientation a ϵ_1/ϵ_2 ratio of 0.515 was initially determined at the mean heat flux point between 1 and 2 A.U. to achieve an antenna temperature of $70^\circ F$. The resulting temperatures at 1 A.U. and 2 A.U. are $125^\circ F$ and $34^\circ F$, respectively. For a 60° orientation, an $\alpha_s = \epsilon_1 = 0.6$ and a $\epsilon_2 = 0.05$ results in a temperature of $135^\circ F$ at 1 A.U. and $-29^\circ F$ at 2 A.U. These temperatures are well within the structural limits of the antenna and represent a close approximation to the internal temperature requirements.

3.2 ISOTOPIC POWER SUPPLY

A heat balance analysis on the radio isotopic power supply has been performed. The surface temperature of the unit has been calculated as a function of surface emissivity and solar distance. It is concluded that the surface temperature can be held within acceptable limits by properly selecting surface optical properties, as shown in Figure 3-3. The detailed analysis is given in Appendix A.

A thermal analysis has been conducted on the DC-DC converter located originally close to the isotopic power supply. The surface temperature of the unit is determined as a function of the surface emissivity and the converter heat dissipation. The addition of cooling fins has been investigated. It is concluded that the converter must be located where it is not exposed to direct solar radiation and/or the heat dissipation of the isotopic power supply. The results of the study are summarized in Figure 3-4. The analytical details are given in Appendix B.

3.3 MAGNETOMETER AND IONIZATION CHAMBER

Parametric curves have been prepared to allow a quick determination of surface properties required to achieve a desired temperature range as a function of the solar heat flux variation between 1 and 2 A.U., the internal heat dissipation, geometry and orientation. The curves were developed for spheres, cubes and two orientations of a cylinder. The following assumptions were made for all cases:

1. Unit is isothermal
2. Coating properties do not change with time and/or temperature
3. Steady state conditions exist at all times
4. No external effect from surrounding components
5. Emissivity equal to solar absorptivity on sun incident surface
6. Temperature at mean solar flux of 221 Btu/hr. ft^2 is $70^{\circ}F$.

Fig. 3-3 Isotope Power Supply
Surface Temperature

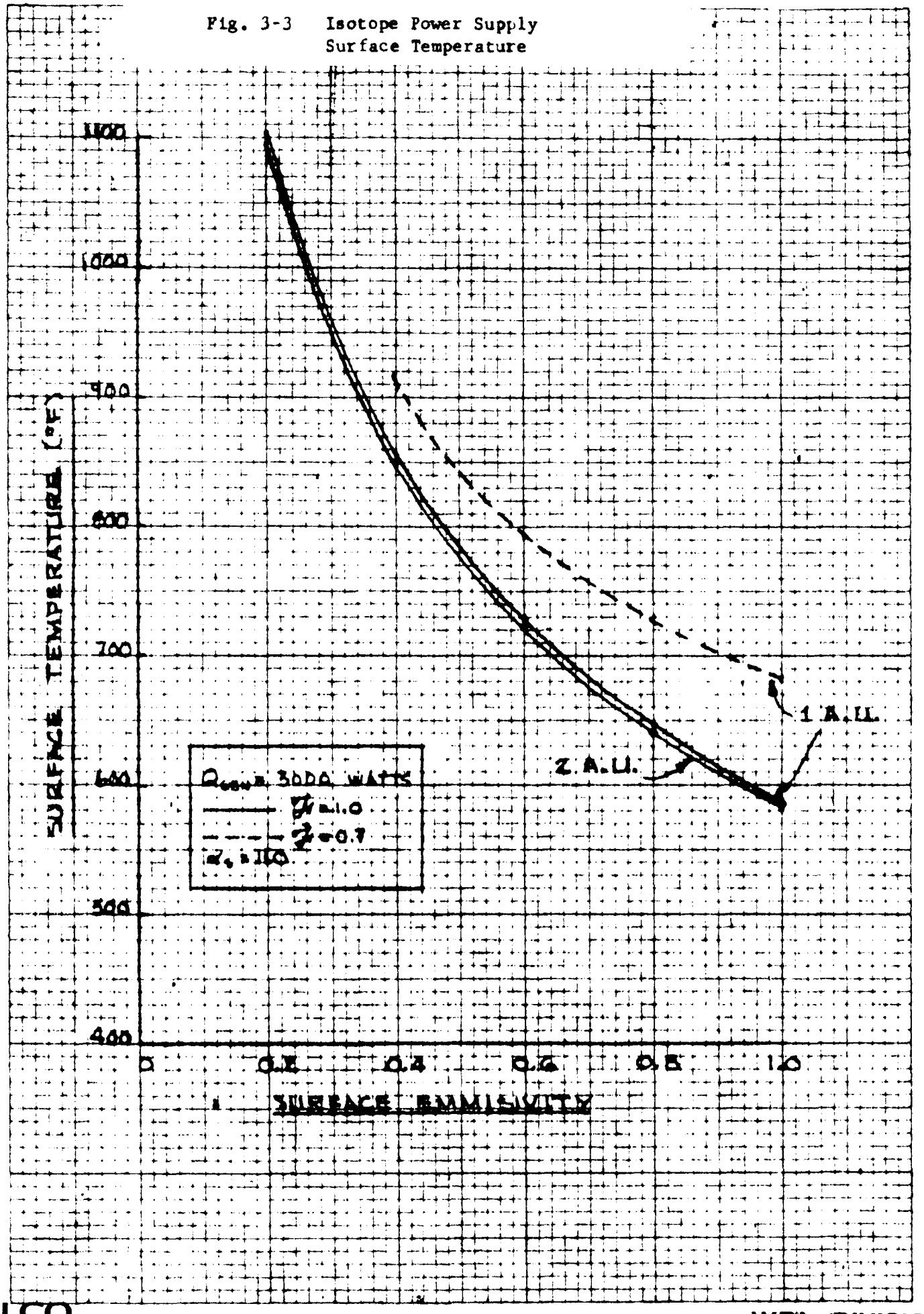

Fig. 3-4 DC-DC Converter - Approximate Surface Temperature

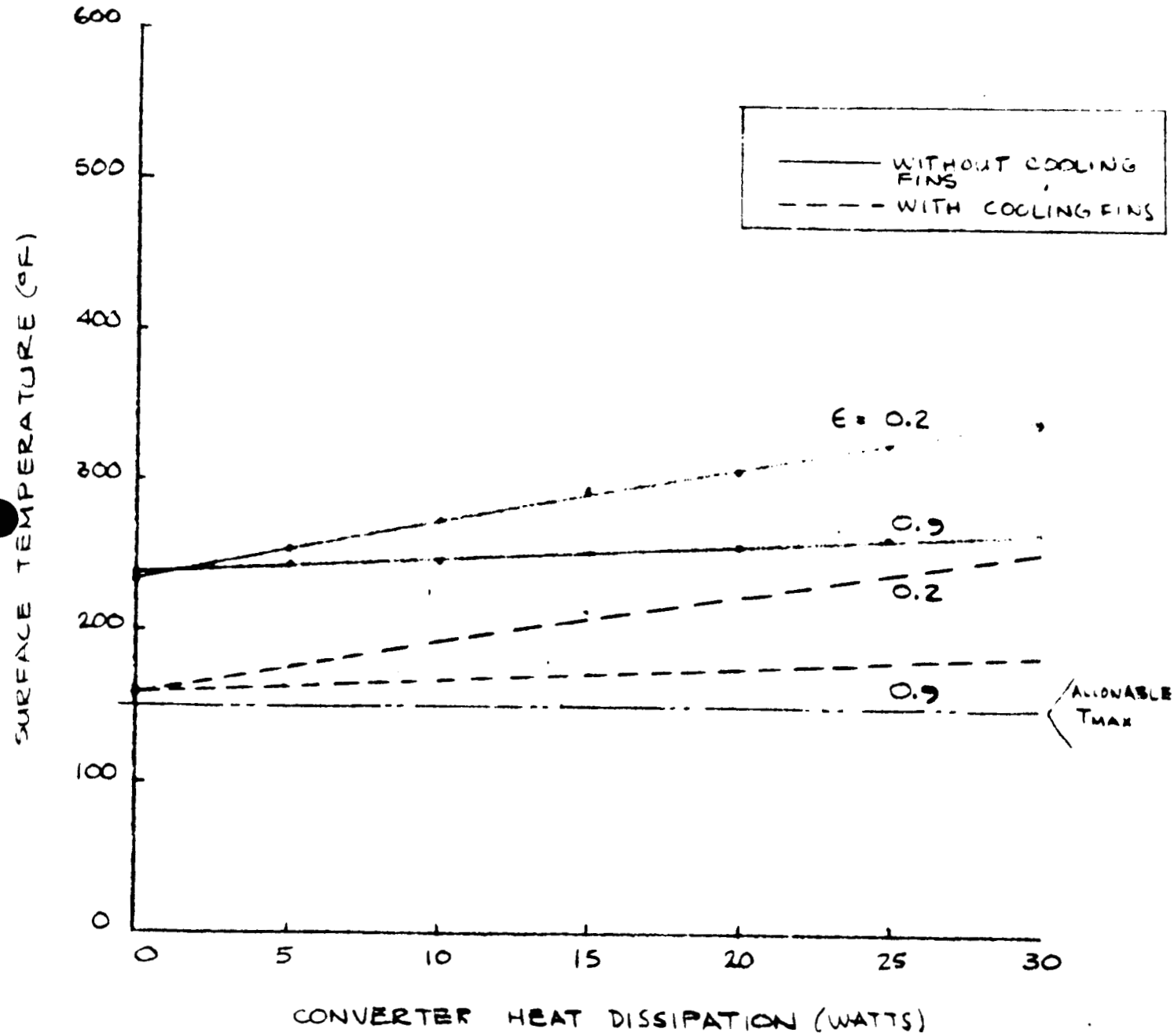

The curves are presented in Figures 3-5 through 3-15. To illustrate the use of these curves, the magnetometer, a cyclinder whose longitudinal axis is perpendicular to the sun rays, and the ion chamber, a sphere, will be used as examples.

3.3.1 Magnetometer System Schematic

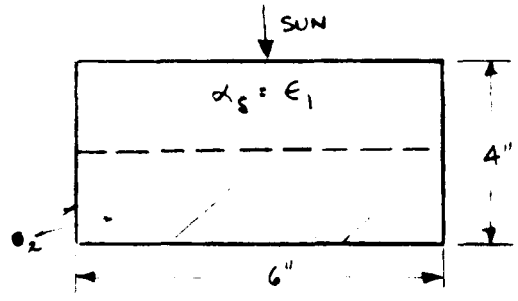

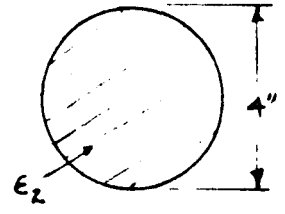

Heat dissipation q = 7 watts

Diameter D = 0.33 ft.

Length L = 0.5 ft.

Temp. limits = 0 to 130°F

Analysis

$$\frac{q}{DL} = 42 \text{ watts/ft}^2; \quad D/L = 0.67$$

From Figure 3-10, $\epsilon_2 = 0.4$; from Figure 3-12 for $\frac{\alpha_s}{E_{cy}} = 0.3$, the temperature at 1 A.U. ($T_{1\ AU}$) is 112°F and the temperature at 2 A.U. ($T_{2\ AU}$) is 51°F. From Figure 3-9, $E_{cy} = 0.95$ and $\alpha_s = \epsilon_1 = 0.285$. If the magnetometer axis is aligned with the sun, the resulting temperatures are 91°F at 1 A.U. and 43°F at 2 A.U., still within the required limits.

3.3.2 Ion Chamber Schematic

The ion chamber surface characteristics can be obtained from Figure 3-5, 3-6, and 3-7. The following geometry has been investigated:

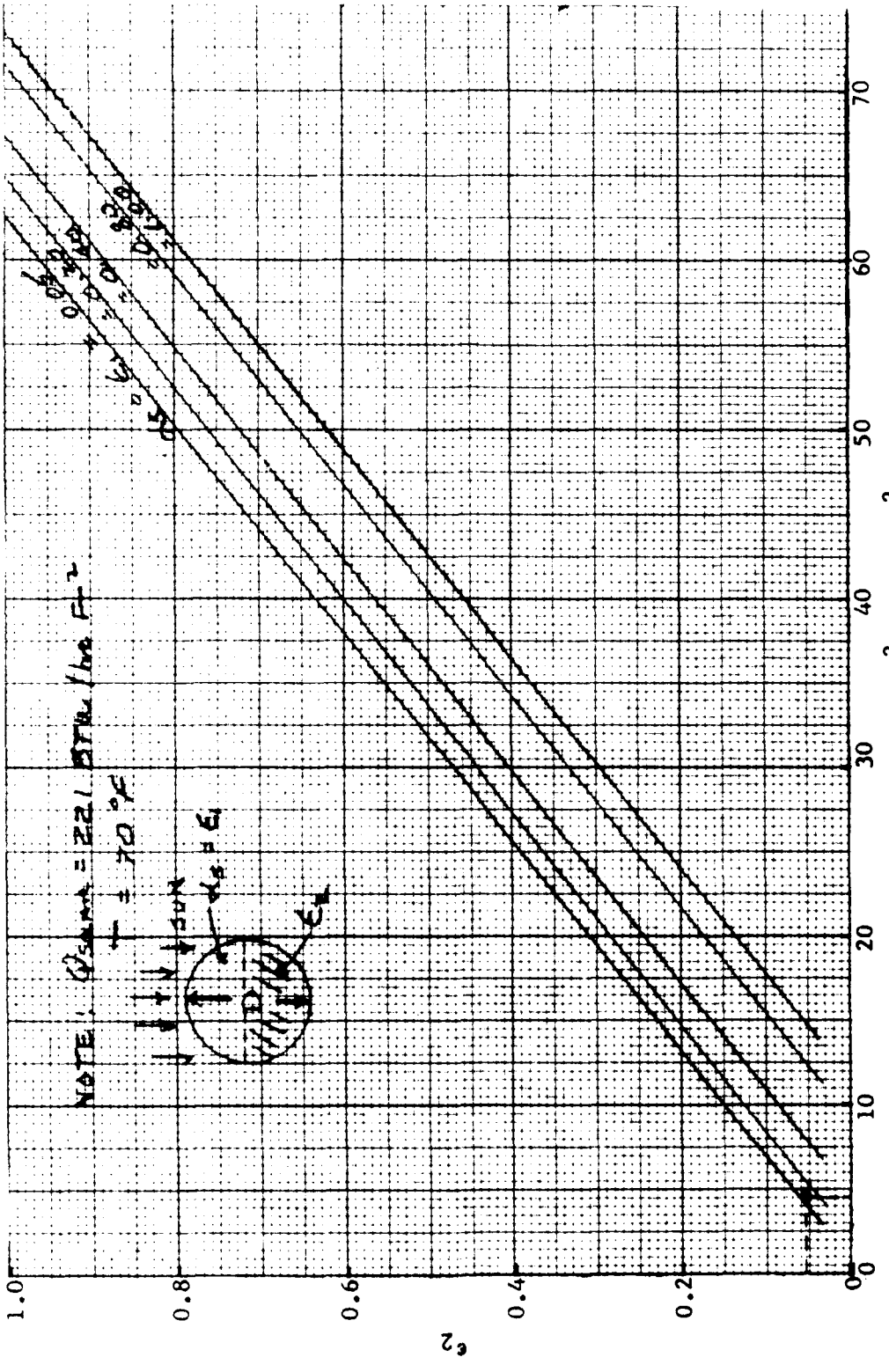

Fig. 3-5 Required Surface Property Combinations to Dissipate a Given Heat Load - Sphere
(Emissivity (ε) equal to absorptivity (α) on sun impinging surface.)

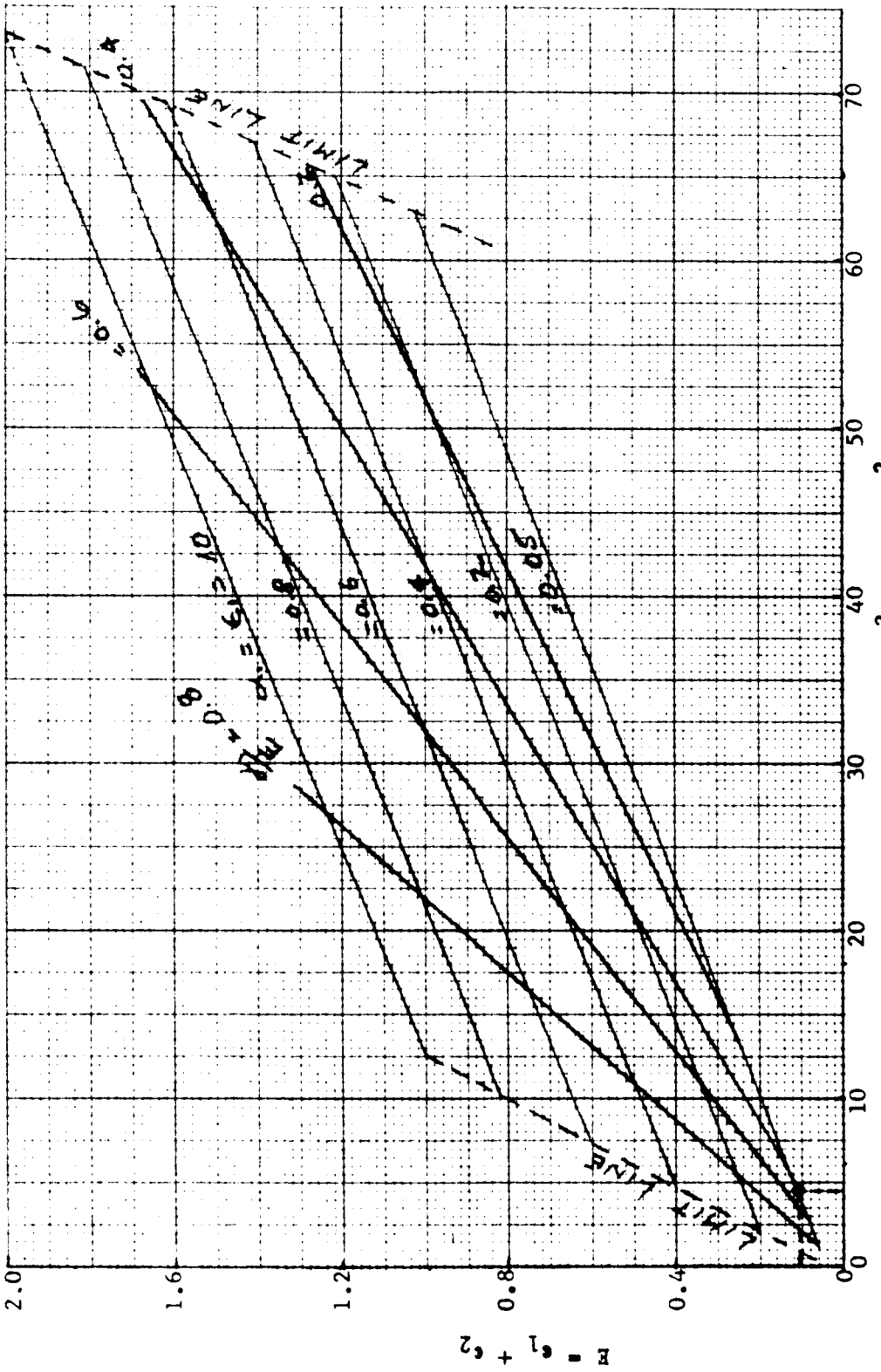

Fig. 3-6 Thermal Characteristics for a Sphere to Achieve 70°F at the Mean Solar Load Between 1 and 2 A.U. as a Function of Internal Heat Generation and Diameter

Fig. 3-7 Temperature of a Sphere at 1 and 2 A.U. as a Function of Surface Properties

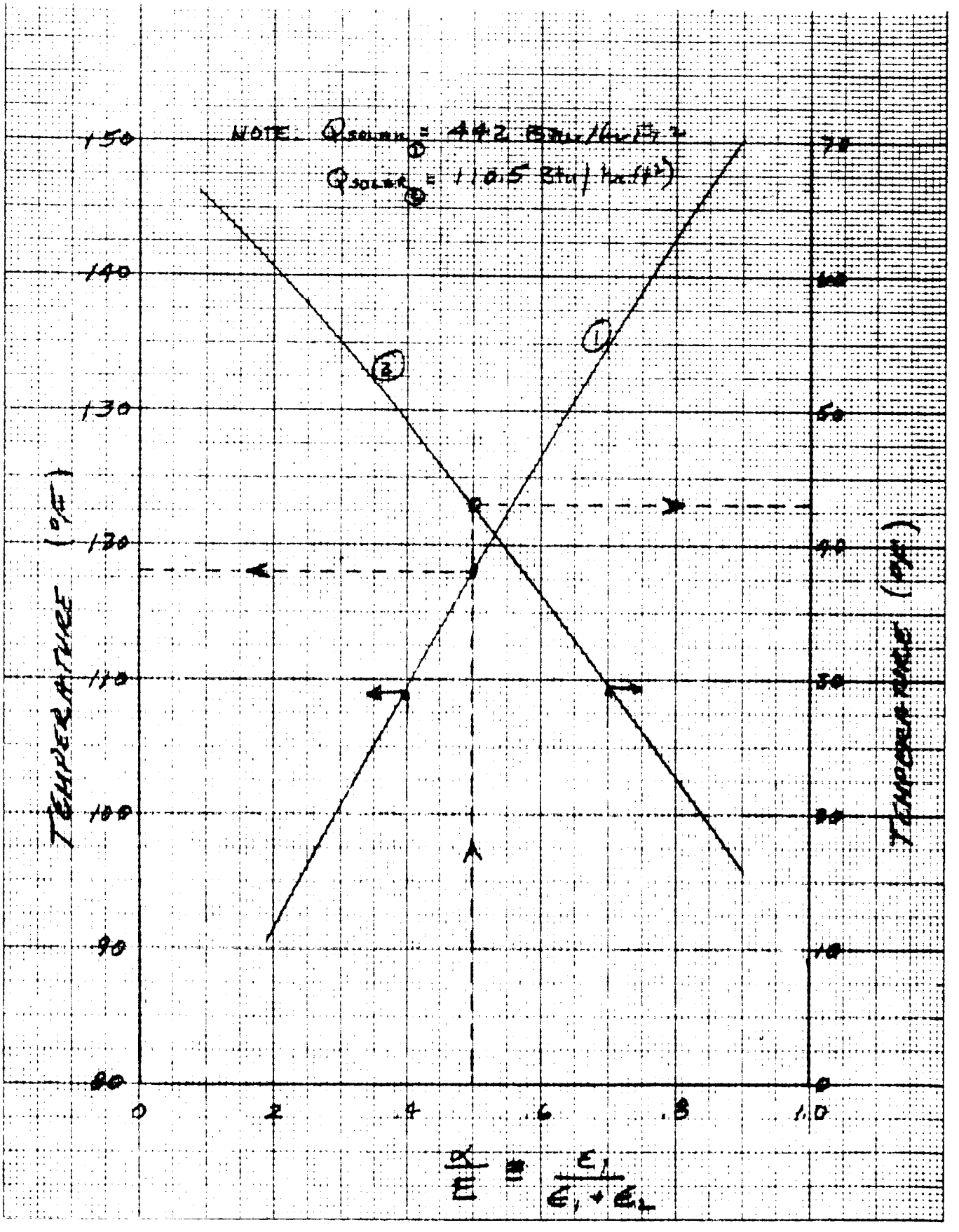

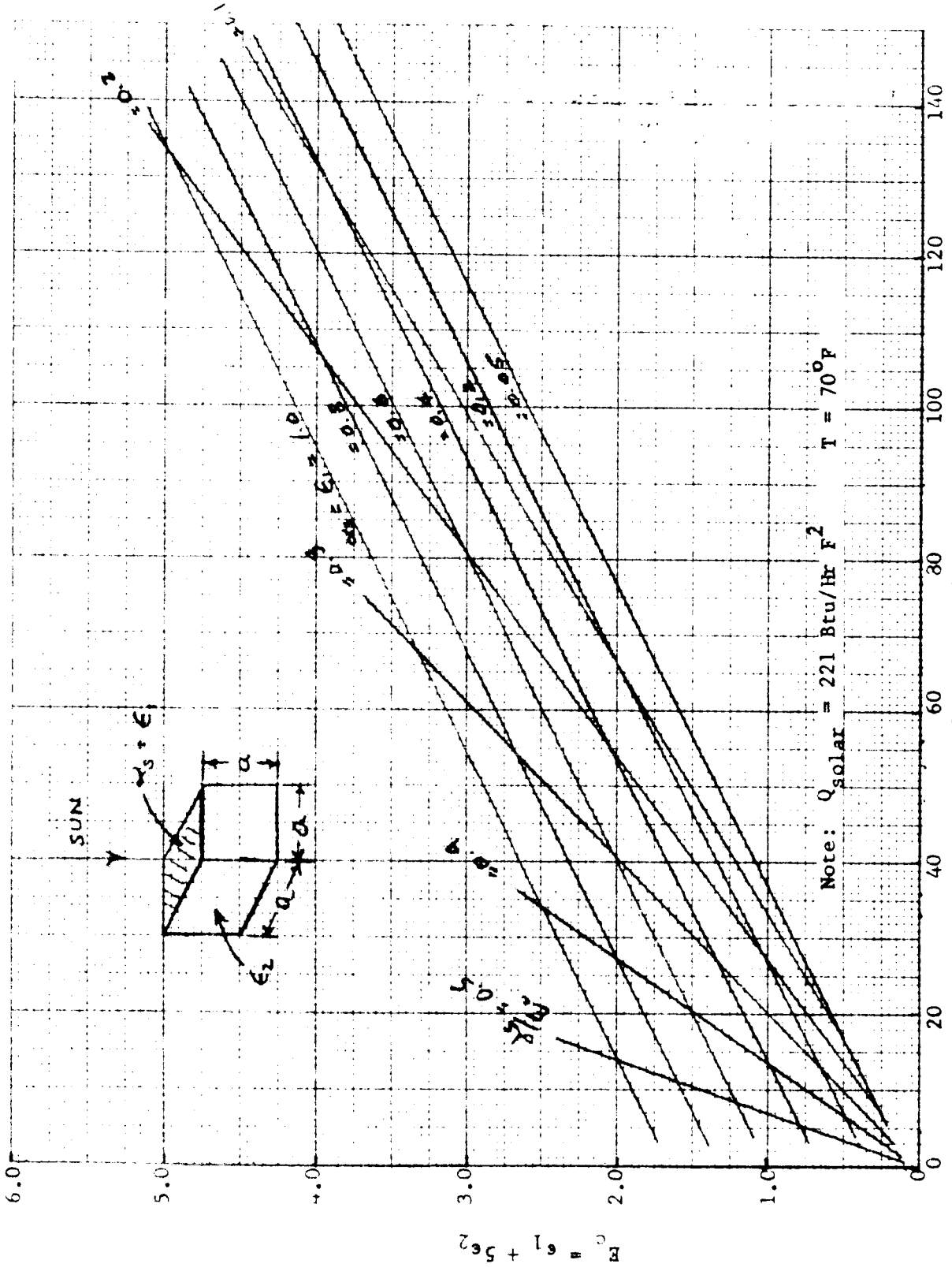

Fig. 3-8 Thermal Characteristics for a Cube to Achieve 70°F at the Mean Solar Load Between 1 and 2 A.U. as a Function of Internal Heat Generation and Side Dimension

Fig. 3-9 Temperature of a Cube at 1 and 2 A.U. as a Function of Surface Properties

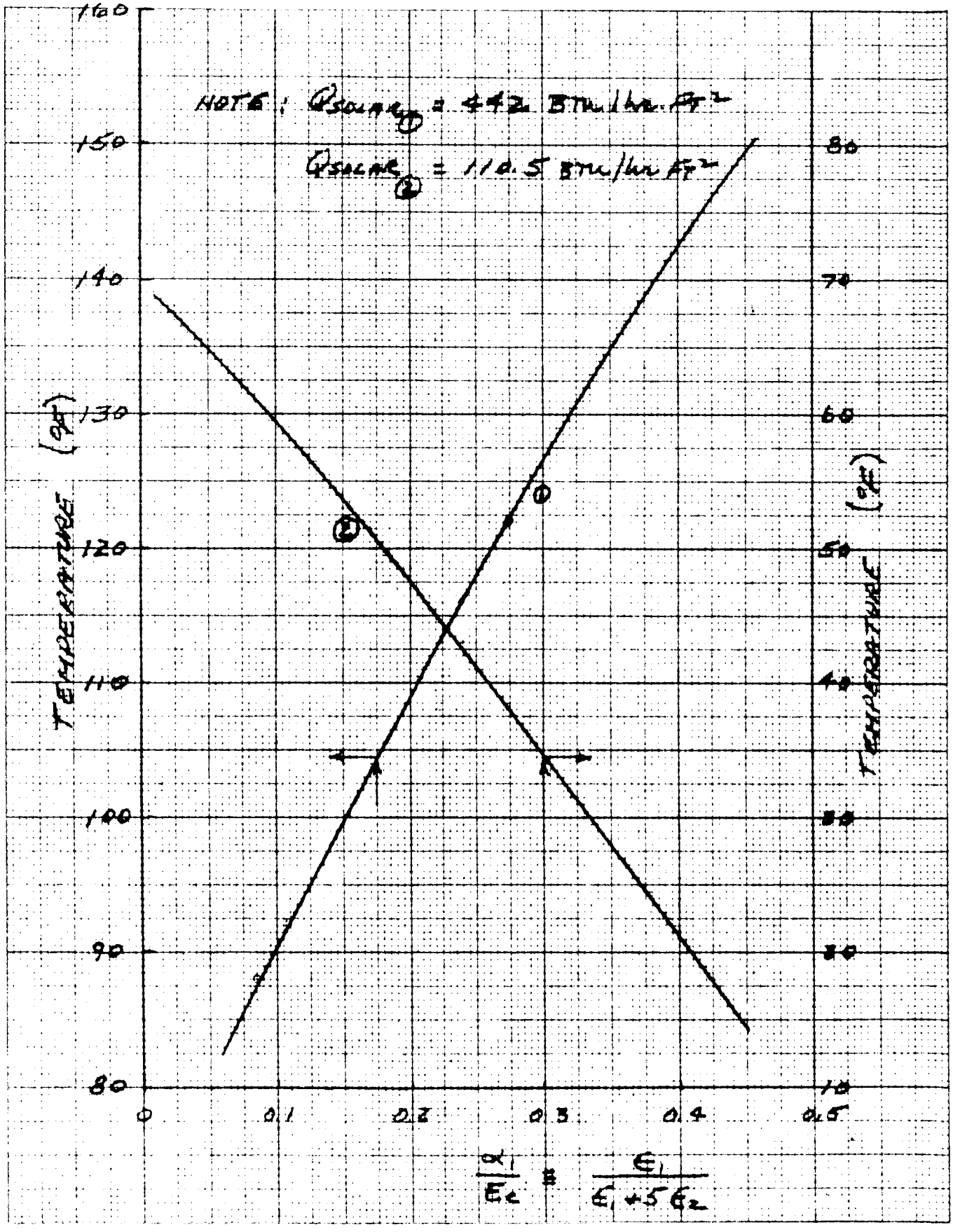

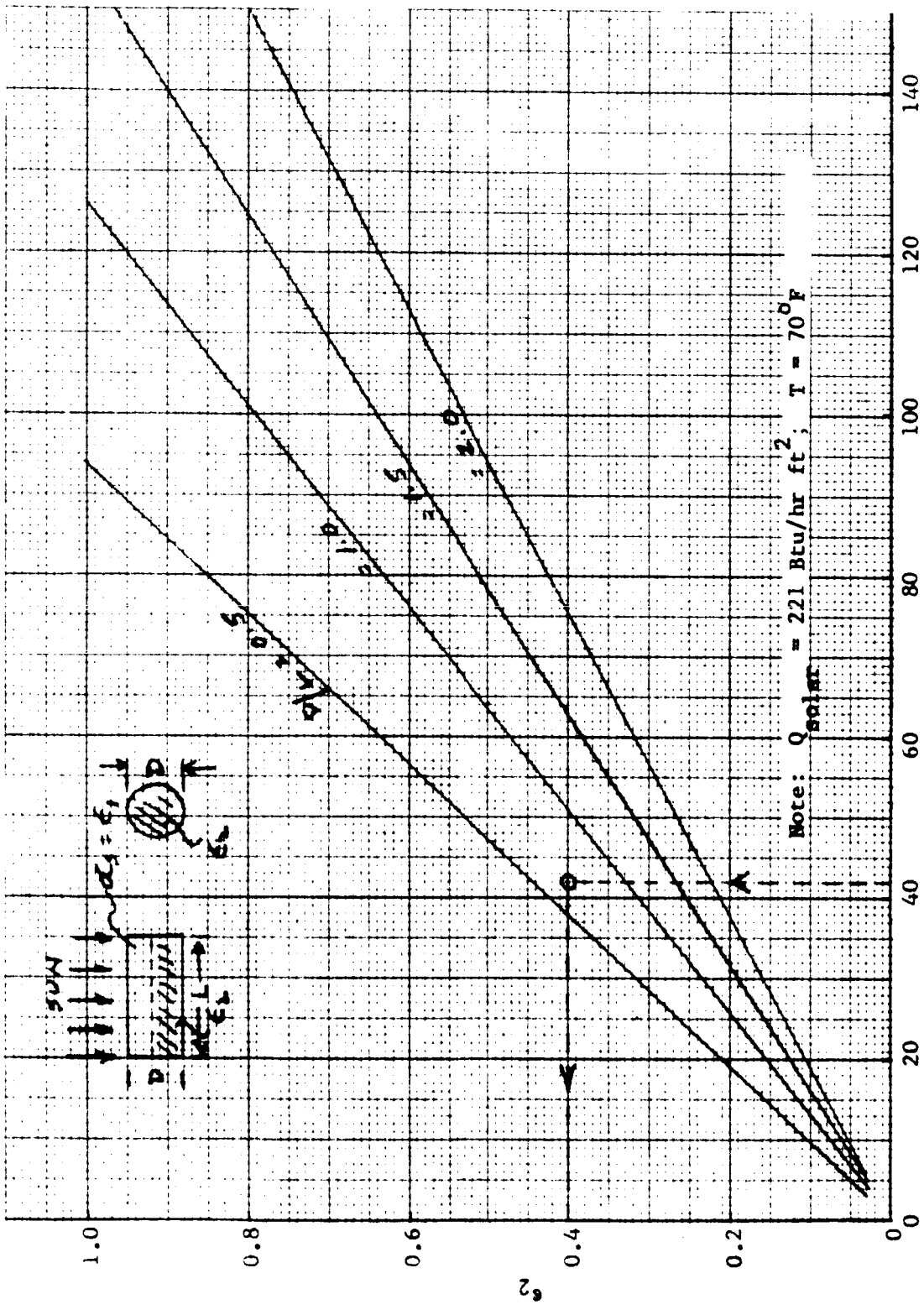

Fig. 3-10 Required Surface Property of Cylinder to Achieve 70°F at Mean Solar Load Between 1 and 2 A.U. as a Function of Internal Heat Dissipation and Cylinder Dimensions

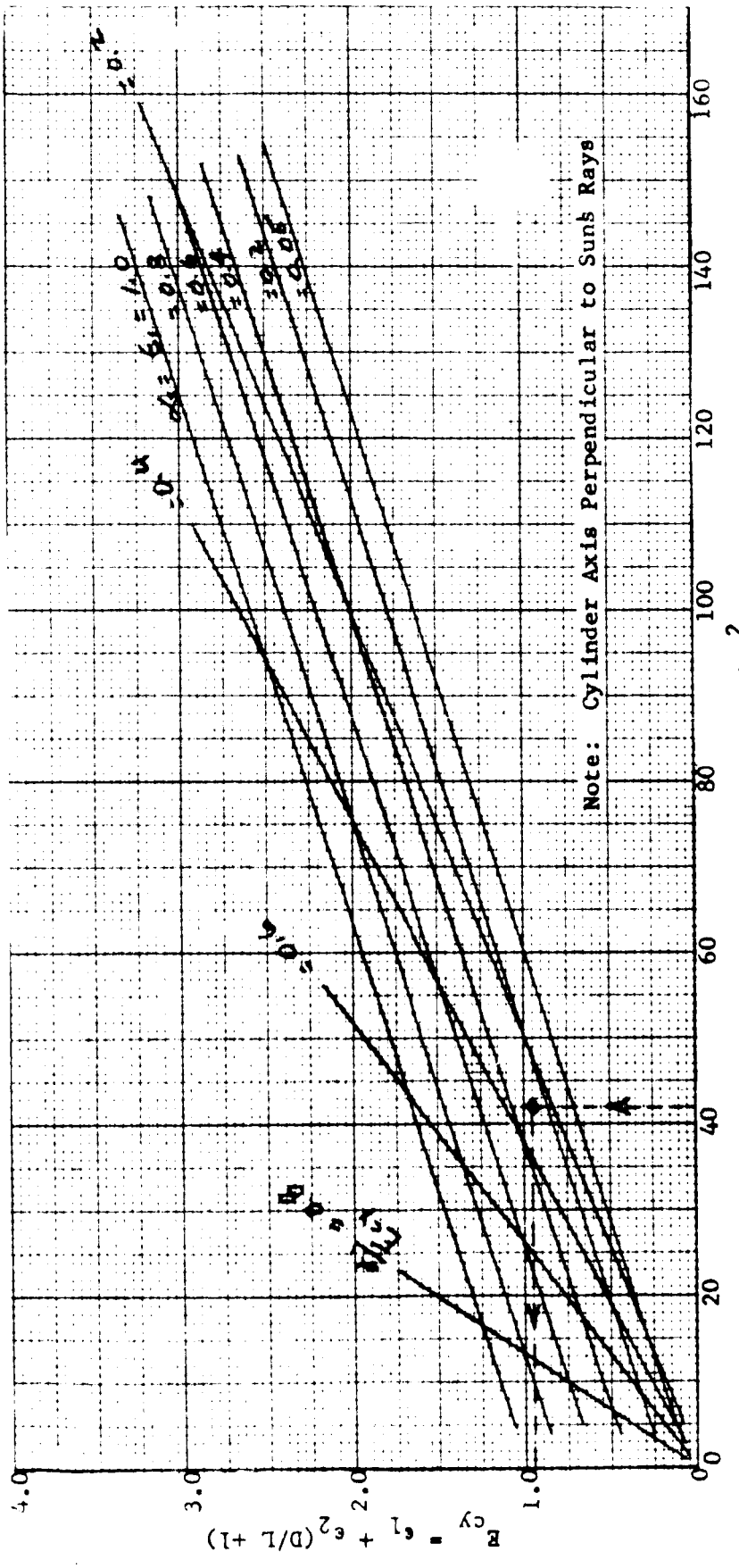

Fig. 3-11 Thermal Characteristics for a Cylinder to Achieve 70°F at a Mean Solar Load Between 1 and 2 A.U. as a Function of Internal Heat Dissipation and Cylinder Dimensions

Fig. 3-12 Temperature of Cylinder at 1 and 2 A.U. as a Function of Surface Properties and Dimensions

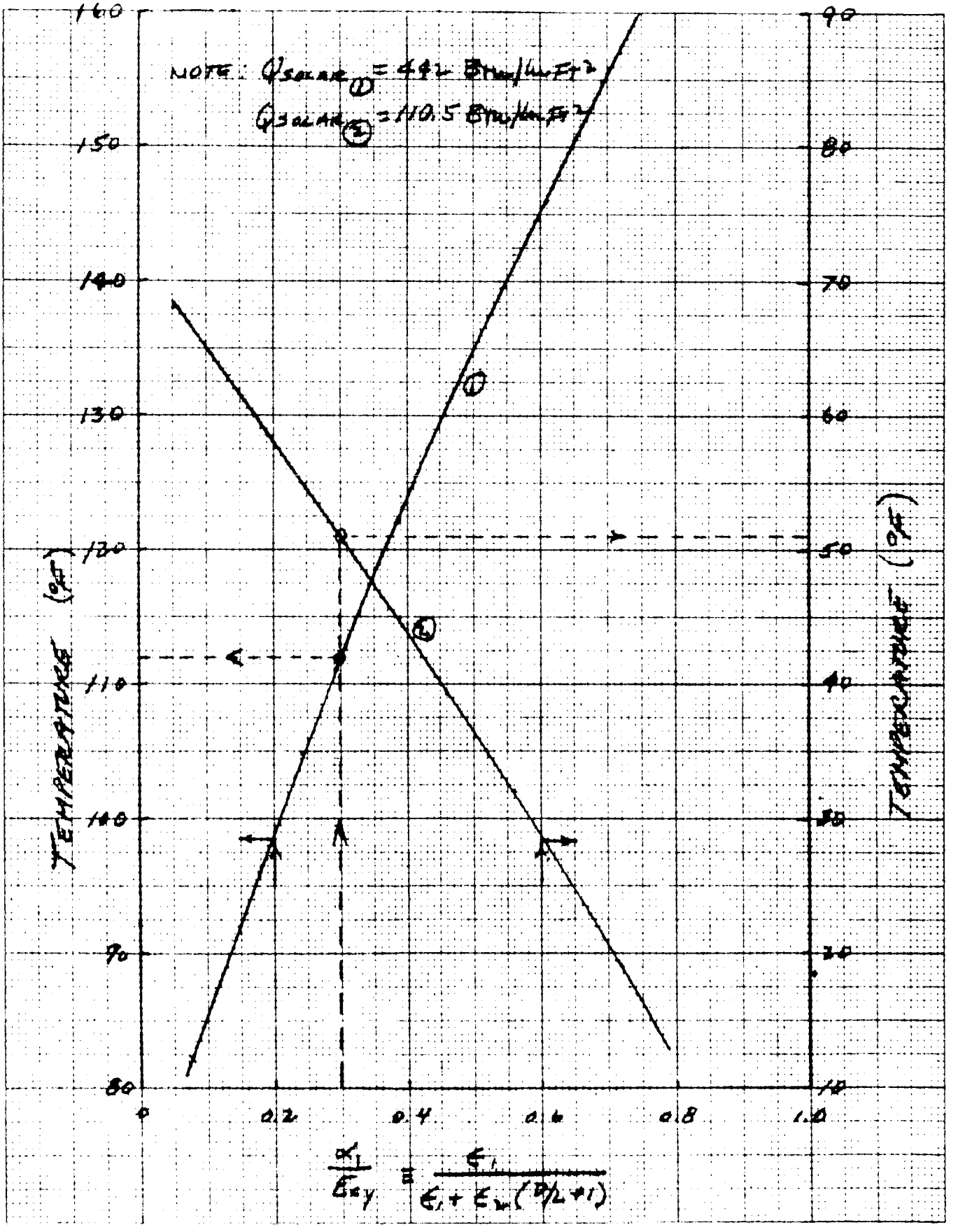

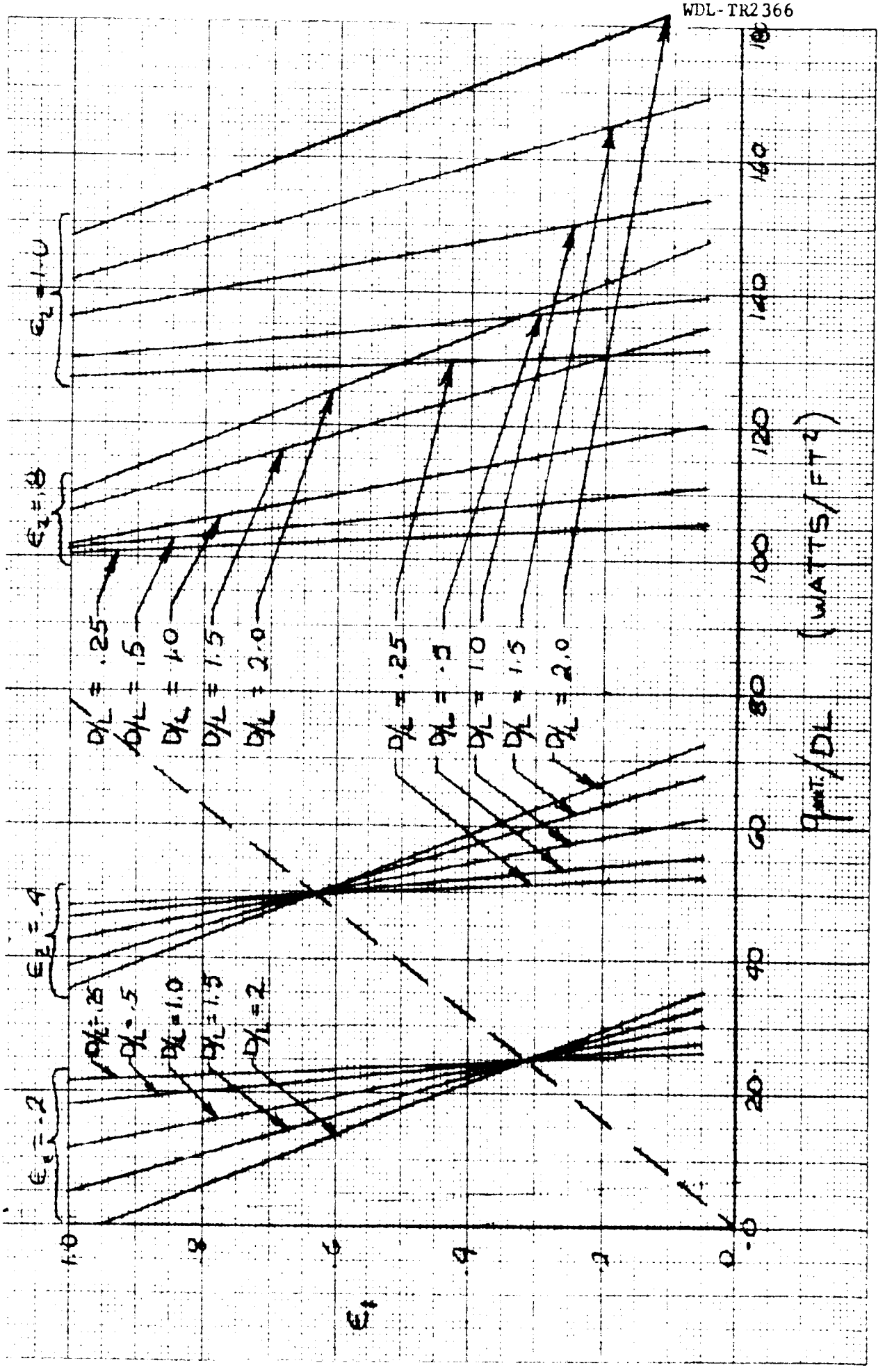

Fig. 3-13 Required Surface Properties of Cylinder to Achieve 70°F at Mean Solar Load Between 1 and 2 A.U.

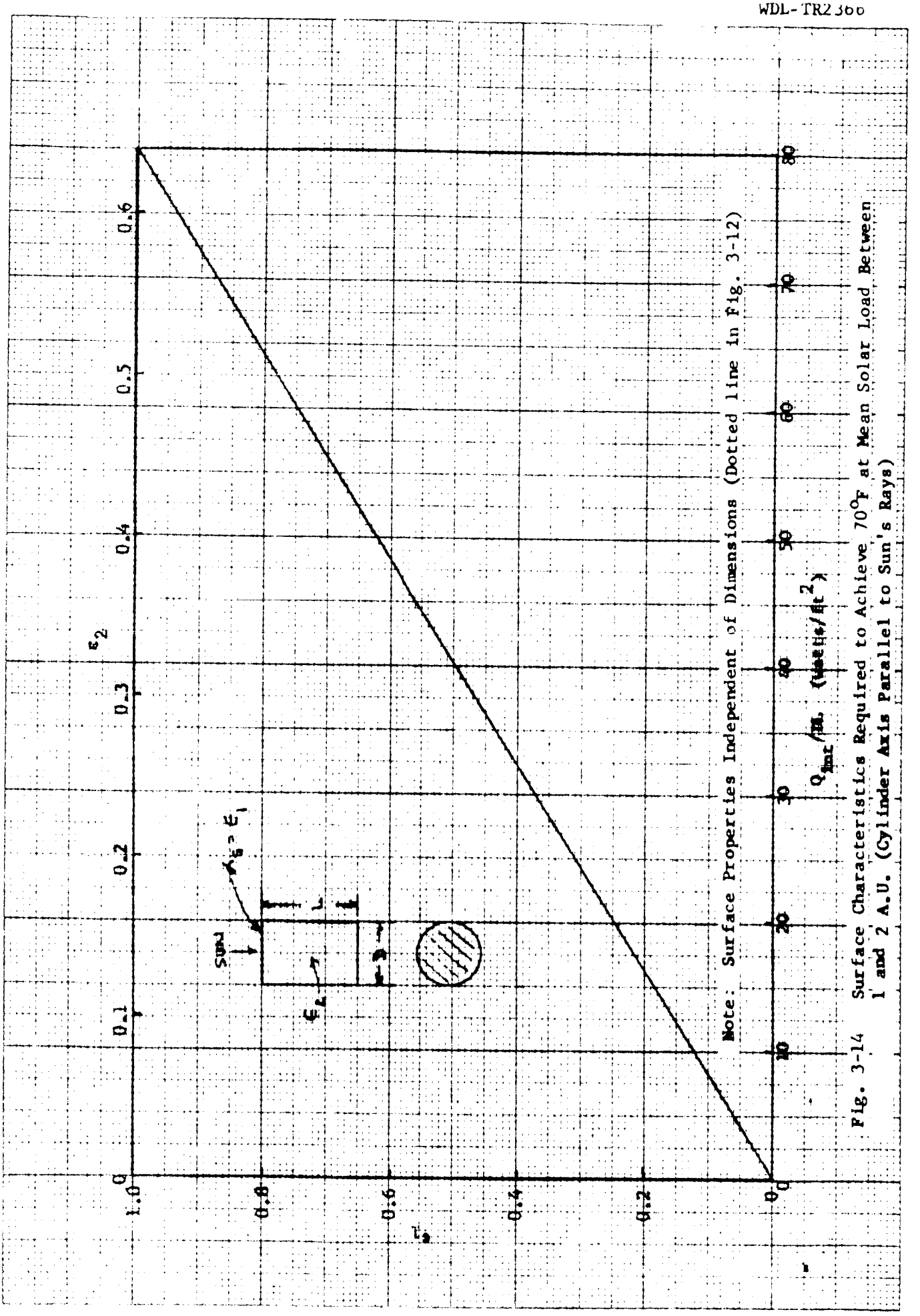

Note: Surface Properties Independent of Dimensions (Dotted line in Fig. 3-12)

Fig. 3-14 Surface Characteristics Required to Achieve 70°F at Mean Solar Load Between 1 and 2 A.U. (Cylinder Axis Parallel to Sun's Rays)

Fig. 3-15 Temperature of Cylinder as a Function of Solar Load for Various Geometries

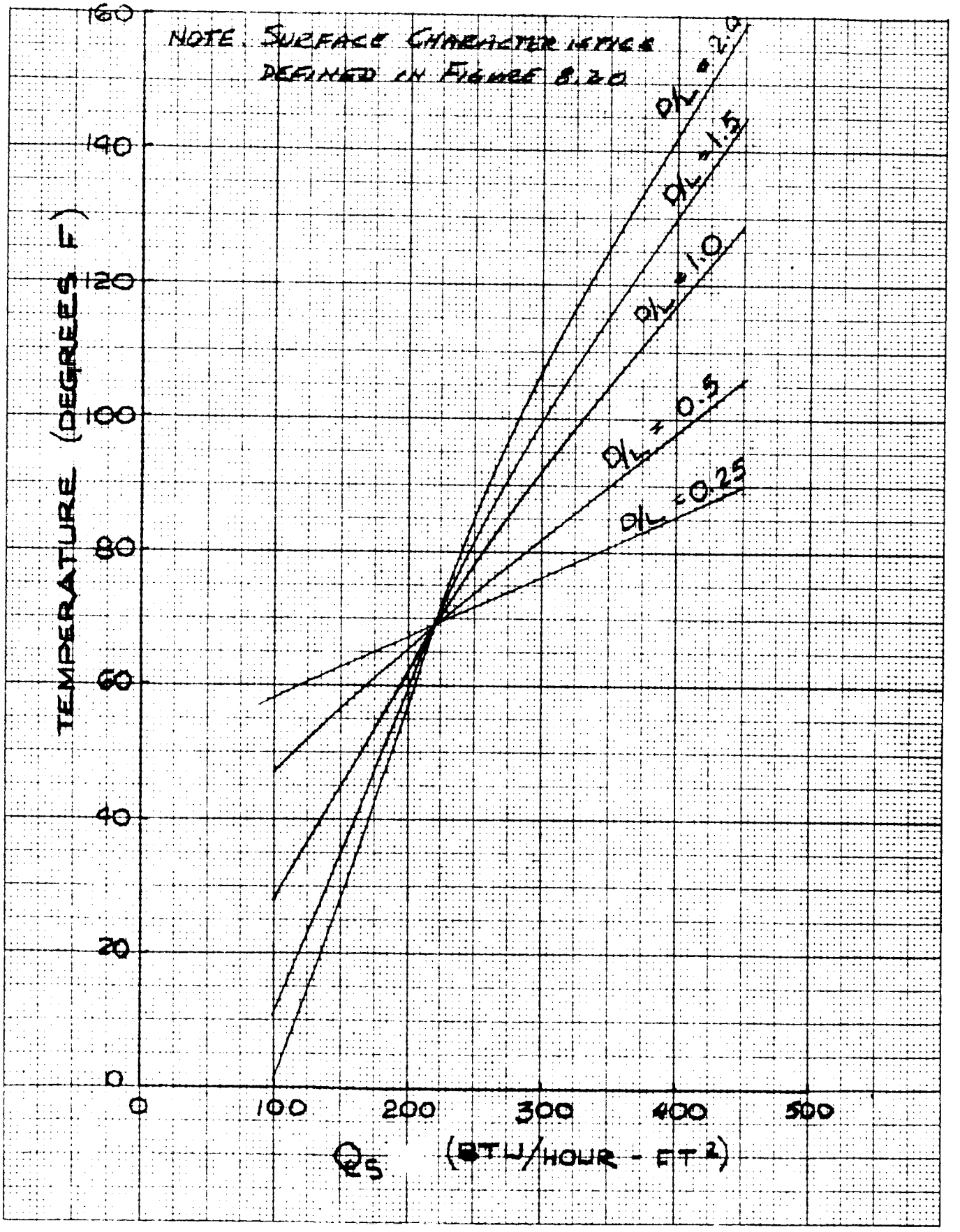

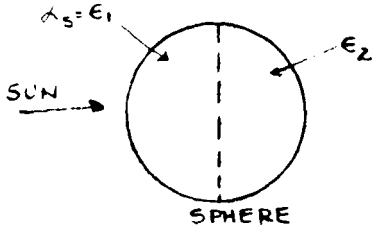

Heat dissipation = 0.5 watt
Diameter = 0.33 ft.
Temp. limits = -22 to +158°F

Analysis

$$\frac{q_{int}}{D^2} = 4.5$$

From Figure 3-7 and assuming $\frac{\alpha_s}{E} = 0.5$ or $\epsilon_1 = \epsilon_2$, $T_{1\ AU} = 118^{\circ}F$ and $T_{2\ AU} = 43^{\circ}F$. From Figure 3-6, $E = 0.11$ and $\alpha_s = \epsilon_1 = \epsilon_2 = 0.055$. From Figure 3-5, $\epsilon_1 = \epsilon_2 = 0.055$ at $q_{int}/D^2 = 4.5$. This result indicates one coating can be used to achieve temperature control for all possible sun look angles.

3.4 SCAN PLATFORM

The scan platform presently contains the UV spectro-photometer, IR radiometer or UV photometers, and slow scan television and is so located as to have solar flux impingement at all times. Two possible thermal configurations were investigated as follows:

System Schematics. The internal heat generation as given in Table 1-1 for the components totals to 24 watts. The temperature limits are 0 to 120°F. The platform is assumed isothermal and totally divorced from the spacecraft. In the case of the unit without the shield, two solar projected areas have been investigated because the orientation could result in two sides having sun impingement.

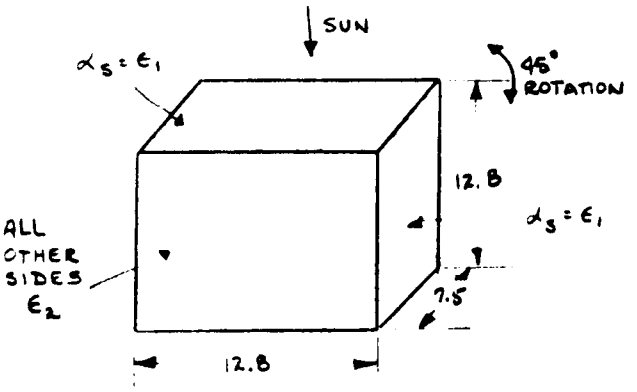

(1)

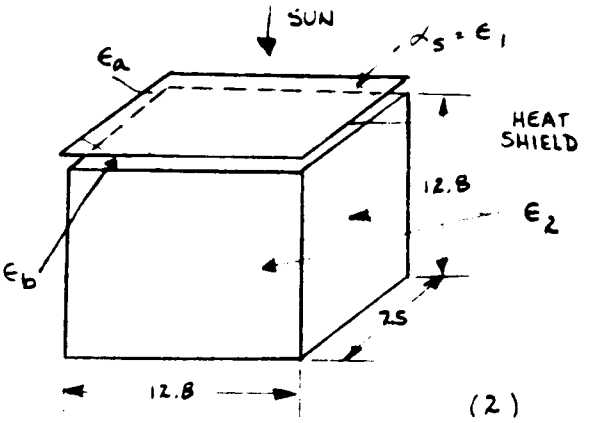

(2)

$\alpha_s = \epsilon_1$ - Outside heat shield surface

ϵ_a - Inside heat shield surface

ϵ_b - Top surface of unit

ϵ_2 - All other surfaces

Separation distance between shield and unit is small enough to make view factor unity.

Analysis

Case 1: Unit Only.

The heat balance equation simplifies as follows:

$$T = \left[\frac{\alpha_s Q_s / r^2 \, A_p + Q_{int}}{\sigma(\epsilon_1 A_1 + \epsilon_2 A_2)}\right]^{\frac{1}{4}} \qquad (3\text{-}2)$$

where

T = temperature of scan unit ($^\circ$R)

$\alpha_s = \epsilon_1$ = solar absorptivity equal ti emissivity

A_p = projected emissivity area - maximum = 0.945 ft^2

- minimum = 0.665 ft^2

Q_s = solar heat flux at 1.0 A.U. = 442 $\frac{\text{Btu}}{\text{hr ft}^2}$

r = solar distance (A.U.)

Q_{int} = internal heat dissipation = 24 watts (82 Btu/hr)

σ = Stefan-Boltzman constant = 0.1713×10^{-8} Btu/hr. ft^2 $(^oR)^4$

ϵ_2 = emissivity surface having no solar impingement

A_1 = maximum area having emissivity ϵ_1 = 1.33 ft^2

A_2 = surface area having no solar impingement = 3.62 ft^2

Case 2: Unit with Heat Shield.

The heat balance equation for the unit temperature becomes:

$$T = \left\{ \frac{A_1 F_e F_a \left[\epsilon_1 Q_s / r^2 A_p + \frac{A_1 F_e F_a Q_{int}}{A_1 F_e F_a + A_2 \epsilon_2} \right]}{\left[(A_1 F_e F_a + A_2 \epsilon_2)(A_1 \epsilon_1 + A_1 F_e F_a) - (A_1 F_e F_a)^2 \right]} + \frac{Q_{int}}{\sigma (A_1 F_e F_a + A_2 \epsilon_2)} \right\}^{\frac{1}{4}} \qquad (3\text{-}3)$$

where

$A_1 = A_p$ = minimum projected area = 0.665 ft^2

F_e = emissivity factor between two plates $\dfrac{1}{\frac{1}{F_a} + \frac{1}{F_b} - 1}$

F_a = view factor between shield and unit = 1.0

The results of the study are tabulated in Table 3-1.

The results indicate that a heat shield design will maintain a closer temperature control than the unit by itself. Assuming power to the unit is off at 1 A.U. and on at 2 A.U., the temperature range for Case 1 is 32° to 121°F or a difference of 89°F, while the heat-shield design Case 2 temperature range is 89°F to 119°F or a difference of 30°F. However, the temperatures at 2 A.U. indicate that a problem may exist just prior to turning the components on, -49°F for Case 1 and -51°F for Case 2. The warm-up time may be critical with regard to performance required at encounter. Therefore, it is recommended that the units be activated at 1.6 A.U. or 60 days

prior to Brooks (2) encounter to maintain both designs above their lower temperature limit of $0^{o}F$. Locating the scan platform behind the bus will require heat to be continuously generated from injection to encounter to maintain temperature control. At 24 watts and surface emissivity of 0.1, the steady state temperature is approximately $98^{o}F$.

TABLE 3-1 Scan Platform Temperature Control

Distance	$\alpha_s = \epsilon_1$	ϵ_2	Unit Temperature (^{o}F)			
			With Internal Heat		Without Internal Heat	
			Max*	Min*	Max	Min
1 A.U.	1.0	1.0	33	0	11	-28
		0.2	153	112	127	78
		0.05	203	158	174	121
With Heat Shield	1.0	1.0	--	-47	--	-91
$\epsilon_a = 1.0$		0.2	--	119	--	58
$\epsilon_b = 1.0$		0.1	--	187	--	119
		0.05	--	221	--	170
2 A.U.	1.0	1.0	-75	-94	$<$-75	$\ll$-75
		0.2	20	-20	-45	-80
		0.05	58	32	-12	-49
With Heat Shield	1.0	0.2	--	32	--	-94
$\epsilon_a = 1.0$		0.1	--	89	--	-51
$\epsilon_b = 1.0$		0.05	--	138	--	-15

* Maximum and minimum projected area

SECTION 4

COATINGS AND MATERIALS

4.1 ENVIRONMENT

During the study, an examination of the effects of ultraviolet and nuclear radiation and of low temperatures on thermal control coatings and materials has been conducted. The study has investigated the degradation in optical characteristics, solar absorptance (α_s) and infrared emittance (ϵ), of coatings and materials when subjected to the estimated space environment. An attempt has been made to establish five α_s/ϵ coatings that cover the complete spectral range and also include coatings that are flat across the spectral range, i.e. $\alpha_s/\epsilon \approx 1.0$, for a wide variation in reflectivities. The preferred coatings are listed in Table 4-1. Examination of the evnironment reveals problems varying from inconsequential to serious, as discussed below.

Table 4-1. Preferred Coatings

DESIGN α_s/ϵ	RECOMMENDED MATERIAL	OBSERVED α_s/ϵ
0.27/0.90 (Solar Reflector)	$ZnO-K_2SiO_4$ (IITRI-Z93)	0.16/0.90
	ZnO-Silicone (IITRI-S33)	0.25/0.80
	$ZnO-K_2SiO_4$ (IITRI-Z108)	0.27/ *
	Kem-M49W-C17	0.26/0.79
0.97/0.96 (Flat Absorber)	Micobond	0.94/0.91
	Kem-M49BC	0.94/0.88
	Laminar X500 Flat Green No. 49-41	0.70/0.84
0.50/0.50 (Medium Flat Obsorber)	SS-316 (Clean and Smooth)	0.45/0.30
	Anodized Al (Ematal)	0.49/0.80
	Rokide on Al	0.54/0.75
	Aluminized Silicone Alkyd (D4D)	0.33/0.34
0.25/0.25 (Flat Reflector)	Fuller 171-A-152	0.22/0.24
	Alumatone	0.20/0.24
0.30/.03 (Tabor Surface)	Gold Plate on Al	0.30/0.03
	SS-321 (polished)	* /0.07
	Multimet (Polished)	* /0.04
	Aluminum 2024	0.27/0.02

*No data could be found.

4.1.1 Temperature

The minimum temperature is probably the most serious environmental constraint of the parameters given. Data is given for some materials, but very low temperature data are sparse.

4.1.2 Solar Constant

Decreasing from 130 watts/ft^2 (one sun) to a low value to 32.5 watts/ft^2; this is no problem.

4.1.3 Ultraviolet

4,000 ESH is a serious problem, eliminating many of the organic and inorganic coatings.

4.1.4 Corpuscular Radiation

The energy deposition, dose rate and total doses are controlled by solar wind protons. The dose of 10^8 ergs/gm is not large, but requires qualification tests for some organic and inorganic coatings. Oxide coatings and metals will be undamaged. No internal problems of any kind exist.

4.1.5 Micrometeoroids

Small size, 10^{-10} gm, $3 \times 10^6/M^2$-Yr. Large size, 10^{-6} gm, $3/M^2$-Yr. There is no micrometeoroid problem in the interplanetary medium. While there will be some pitting and roughening, the area affected will not be large enough to change the values of the optical properties [Streed and Beveridge, 1964; Lehr, Martire and Tronolone, 1962].

4.1.6 Boost Phase

None of the vibrations or "g" forces appear large enough to pose a problem for any of the present high-quality coatings. Room temperature

vibrations conducted by IITRI [Zerlaut and Harada, 1963a] at 15 x 10^{-4} inches/inc, for six minutes at 1,725 cpm, followed by 10 cycles of thermal shock (LN_2 to 200°F) were given to a number of coatings. The SP-500-ZnC coatings passed this test easily.

4.2 THERMAL CONTROL SURFACES

Figures 4-1 to 4-8 and Tables 4-2 to 4-5 present data on candidate materials for temperature control in the five α_s/ϵ categories required.

4.2.1 Solar Reflectors

Four materials appear satisfactory for solar reflectors, with ZnO-K_2SiO_4 (as IITRI-293) and ZnO-silicone (as IITRI-S33) the best. Data are presented in Tables 4-2 and 4-3 and Figures 4-1, 4-2 and 4-3. There are no nuclear radiation data on the IITRI coatings, and this would have to be checked experimentally. It is believed that they will pass. The Kemacryl M49W-C17 passed a severe nuclear radiation test, and the IITRI-2108 passed a limited ultraviolet test (1,700 ESH). Data on Fuller 517-W-1 show it to be inadequate for one property; this being thermal shock. Otherwise, this is a good coating.

4.2.2 Flat Absorbers

Data on three materials are presented in Table 4-4. The two organics Microbond and Kem-M49BC are essentially undamaged by 630 ESH of ultraviolet, but this is far less than the environment of 4,000 ESH. No low temperature data could be found and the materials should be tested. LMSC has had loosening of Dow 17 bonds to metal, under acrylic paints, after thermal shock tests. The Laminar X500, flat green No. 49-41 manufactured by Magna Coating and Chemical Co. of Los Angeles, is a polyurethane 2 part sprayed-on system with a room temperature cure. After about 600 U.V. sun hours, the visible color changes but the overall spectrum is changed very little. This paint is used on the Mariner Mars 1964 spacecraft.

EFFECT OF UV ON WHITE COATINGS
[AFML, 1964]

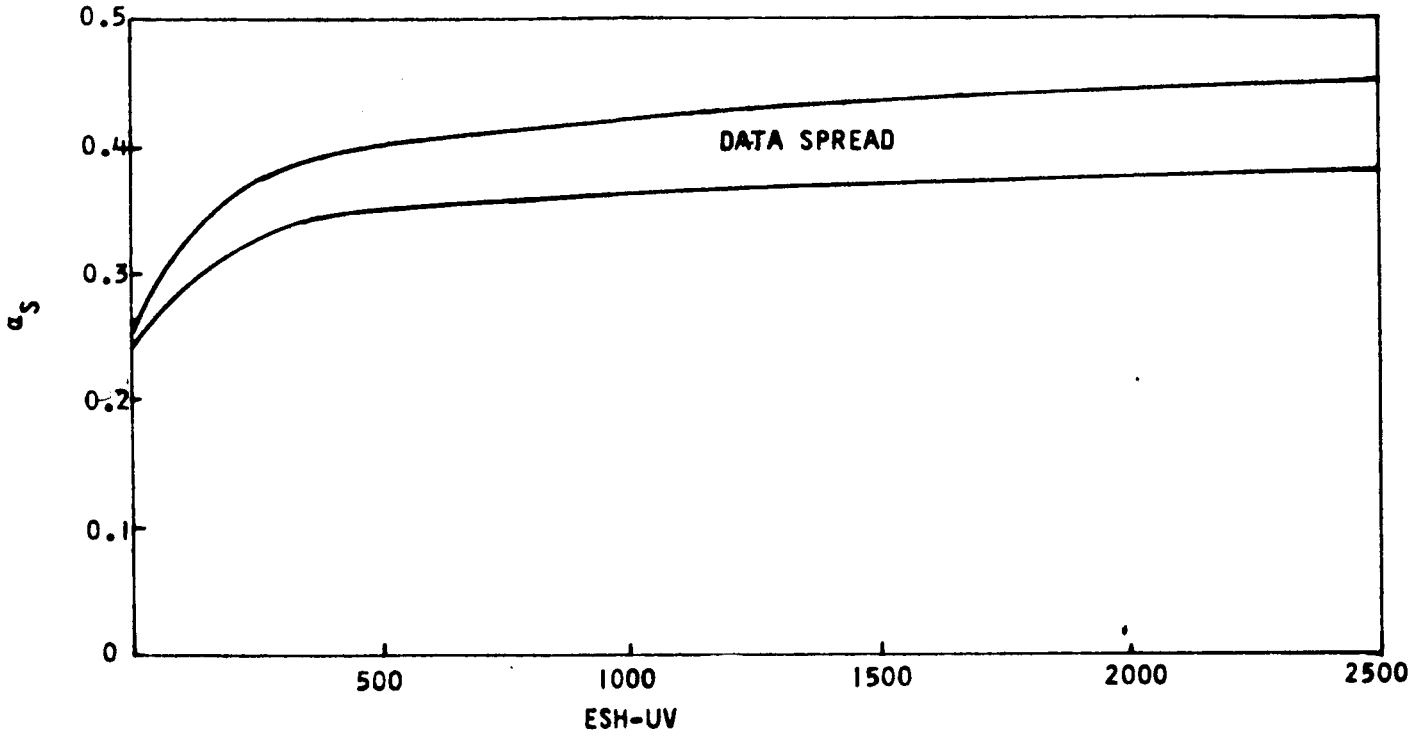

FIG. 4-1 WHITE KEMACRYL

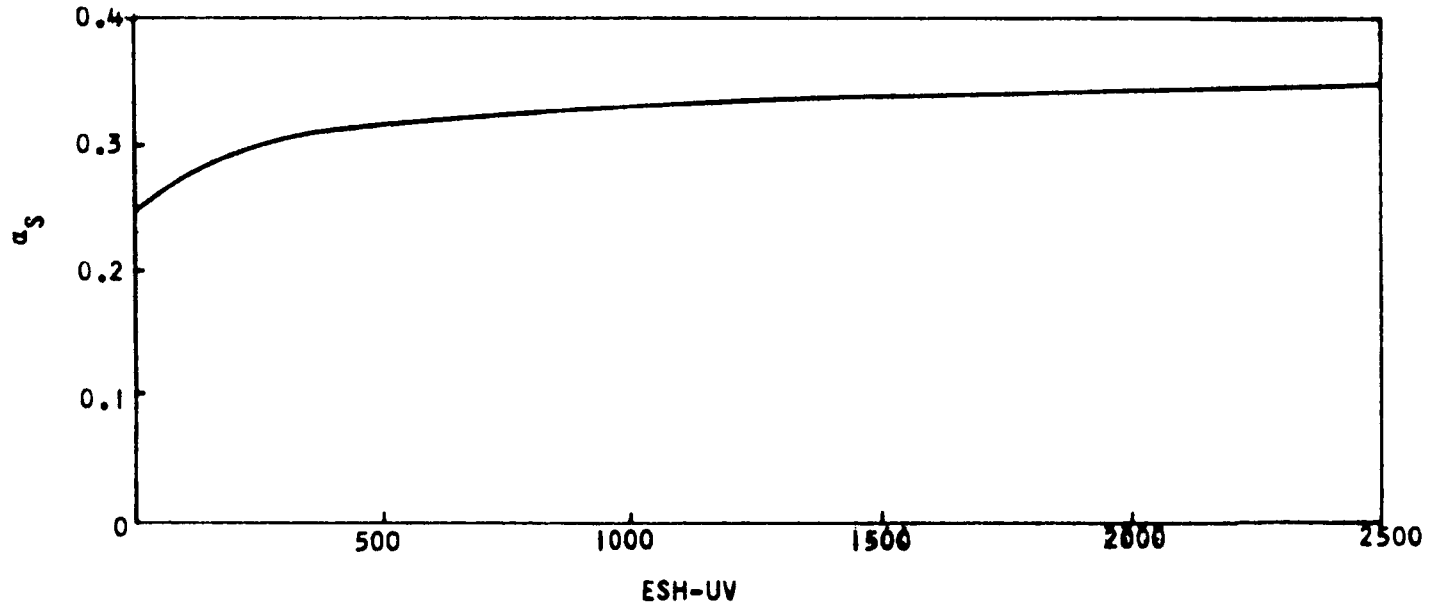

FIG. 4-2. FULLER 517-W-1 GLOSS WHITE ON 6061 ALUMINUM

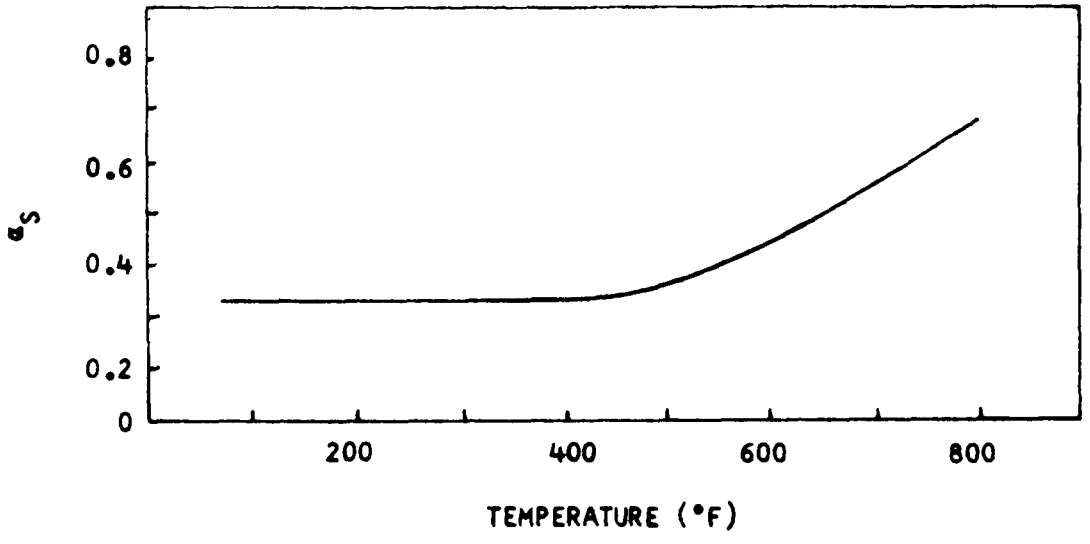

FIG. 4-3 FULLER 517-W-1 GLOSS WHITE PAINT [AFML, 1964]

CONDITIONS: SUBSTRATE 6061 ALUMINUM AND DOW 17 COATED HM21 A MAGNESIUM (NO DIFFERENCE IN RESULTS)

TEST DATA AT 5 mm AND 10^{-3} mm Hg (NO EVIDENCE OF EFFECT DUE TO THE VARIATION IN PRESSURE)

DATA AT TWO TIME EXPOSURES FOR EACH TEMPERATURE:

120 SEC

900 SEC

(SLIGHT INCREASE IN α_S FOR 900 SEC)

LIQUID NITROGEN IMMERSION RESULTED IN COMPLETE LOSS OF BONDING, SURFACE CRACKED AND PEELED

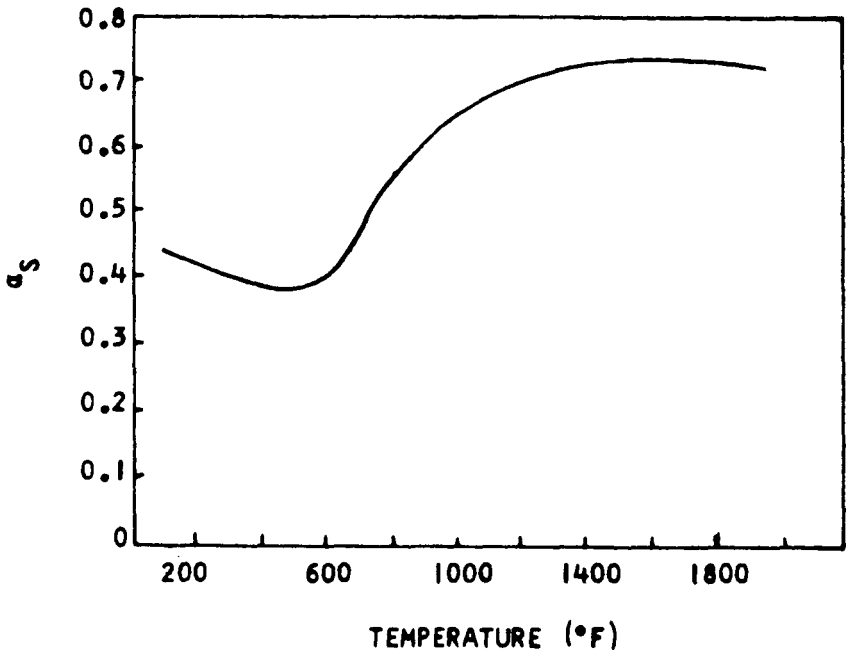

FIG. 4-4 α_s FOR STAINLESS STEEL 316
[WOOD, DEEM, AND LUCKS, 1962]

CONDITIONS: CLEAN AND SMOOTH
MEASURED IN AIR AT 100° F

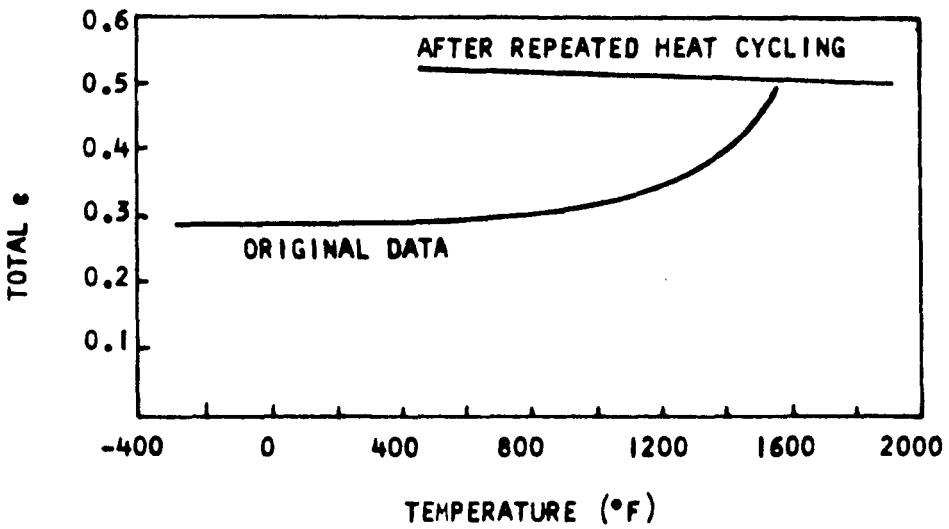

FIG. 4-5 ε FOR STAINLESS STEEL 316
[WOOD, DEEM AND LUCKS, 1962]

CONDITIONS: CLEAN AND SMOOTH
MEASURED IN HELIUM

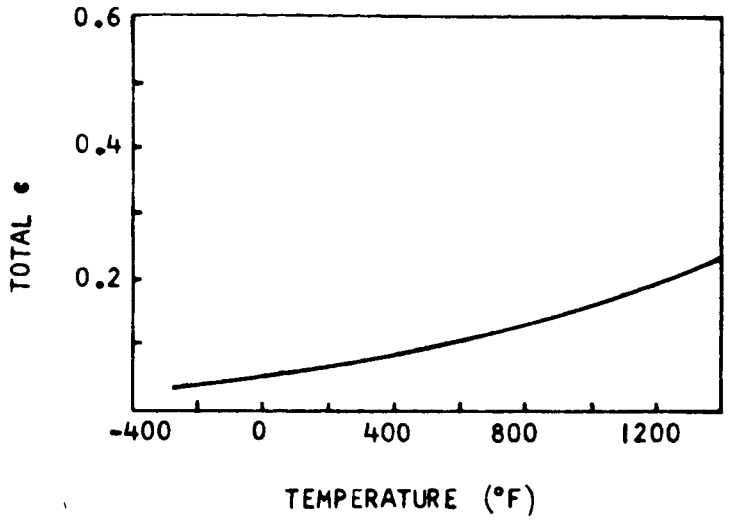

FIG. 4-6 TOTAL ε FOR MULTIMET (ALLOY N-L55)

CONDITIONS: MEASURED IN VACUUM
VERY LITTLE DIFFERENCE
WHEN POLISHED OR OXIDIZED

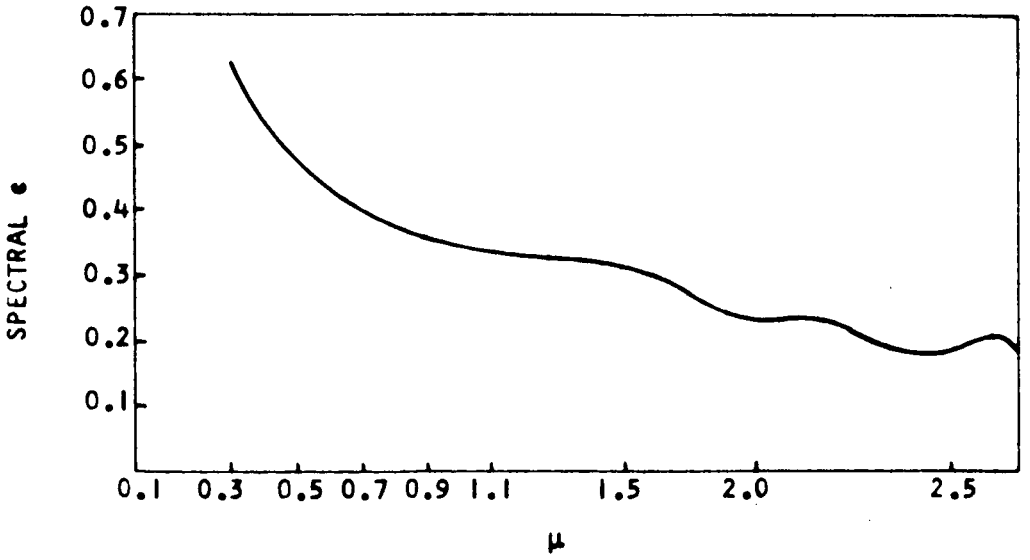

FIG. 4-7 SPECTRAL ε FOR MULTIMET (ALLOY N-155)

CONDITIONS: POLISHED SURFACE
MEASURED IN AIR, ROOM TEMPERATURE

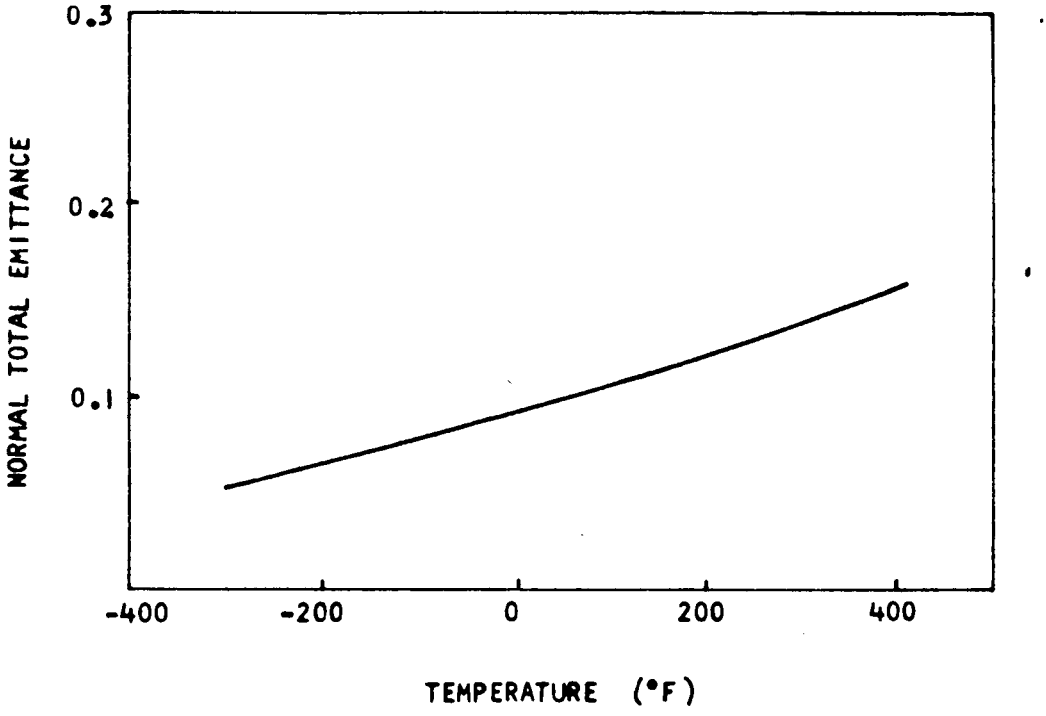

FIG. 4-8 NORMAL TOTAL EMITTANCE OF SS-TYPE 321 VS TEMPERATURE [AFML, 1964]

6 MICROINCHES rms - PROPERTIES MEASURED IN VACUUM

Table 4-2. Effect of UV on White (α_s/ϵ = .27/90) Coatings

[Zerlaut and Harada; 1963b, 1963c]

IITRI-Formulation			Exposure		
No.	Pigment	Cure	ESH	α_s	ϵ
S-33	ZnO	16/700°C	0	.25	.80
	SP-500		4,200	.28	--
Z-93			0	.16	.90
			4,200	.18	--
Z-108	SnO	16/700°C	0	.270	--
	SP-500		1,700	.276	--

Table 4-3. Effect of Radiation on White (α_s/ϵ = .27/.90) Coatings

[AFML, 1964]

Material Description	Exposure ESH-UV	α_s	ϵ	Gamma R	α_s
Kem-M49W-C17 (on Dow 17 on HM21A)	0	.26	.79	0_8	.26
Kem-M49W-C17 (on Dow 17 on HM21A)	150	.32	.80	2×10^8	.32
Kem-M49W-C17 (on Dow 17 on HM21A)	600	.37	.82	---	---
Sod. Silicate "D" plus Ultrox	0	.29	.91	---	---
Sod. Silicate "D" plus Ultrox	700	.29	.85	---	---
Ful. Leaf A1-171-A	0	.21	.16	---	---
Ful. Leaf A1-171-A	600	.30	.20	---	---

Table 4-4. Effect of UV on Black (α_s/ϵ = .96/.96) Surfaces

[Wood, Deem and Lucks, 1962; AFML, 1964]

Material Description	Exposure ESH	α_s	ϵ
Micobond on Dow 17 on HM 21A	0	.94	.91
	630	.98	.87
Kem-M49-BC12 (Same Substrate)	0	.94	.88
	630	.92	.84
Laminar X500, Flat Green No. 49-41	600	.7	.84

Table 4-5. Absorptivity-Emissivity Values

Material	Surface or Substrate	α_s	ϵ
Al 2024	Not reported	.27	.02
Al 6061	Not reported	.41	.04
Av Plate	On Al	.30	.03
Av Vac. Dep.	On Al	.24	.04
SS-302	Polished	.50	.15
Ni (Electroless)	Not reported	.45	.17
Mg	Dow 15	.19	.08
Mg	Dow 1	.64	.53
Mg	Dow 10	.89	.85
Mg	Heavy HAE	.75	.75
Al	Grey anodized	.62	.72
Al	Grey anodized	.53	.50
Mg	Not reported	.72	.82
Rokide	Not reported	.54	.75
Rokide A	Not reported	.21	.80
SiO_2 (5 mils)	Not reported	.21	.83
SiO_2 (5 mils)	Not reported	.15	.90
Fuller 171-A-152	Not reported	.22	.24
MMM-Y9184	Not reported	.26	.03
Dow 17	Mg-AZ31	.59	.54
Ag Plate	Epoxy-Glass	.24	.06
SS-446	No. 1 finish	.53	.43
SS-446	No. 8 finish	.44	.45
SS-316	Clean and smooth	.45	.30
Anod. Al	Ematal process	.49	.80

[Sibert, 1961; MMM, undated; Shipley and Thostesen, Betz, Olson, Schwin and Morris, 1958; Hultquist and Sibert, 1964]

4.2.3 Medium Flat Absorbers

Data on three materials are presented in Figures 4-4 and 4-5 and Table 4-5. The anodized aluminum was made by the Ematal Process, using 33 moles Na_3PO_4 per mole of H_3PO_4. Non-leafing aluminum paints were rejected because of their inability to take thermal shock. The stainless steel 316 should withstand all of the Comet Probe environments. Very little data was available on a G.E. composite, aluminum in a silicone alkyd (D4D) though it indicates the best performance of the four coatings.

4.2.4 Flat Reflectors

The best prospect for this application is Fuller 171-A-152 Table 4-5. LMSC formulations (PB-55) of this product are under test at LMSC, and unpublished data indicate that it may take all of the environments except perhaps the low temperature. New LMSC formulations, involving experimental silicones and non-leafing aluminum, show promise of being better flat reflectors. The alumatone developed by the Chromatone Co. is an aluminum sigmented petrol resin presently used on the Interim Communications Satellite for ASD.

4.2.5 Tabor Surfaces

Four materials are recommended for Tabor surfaces: Aluminum 2024, polished 321-SS, polished Multimet, and gold plate on aluminum. There should be no problem with any of these surfaces. Optical property data are presented in Table 4-5 and Figures 4-6 and 4-8. An additional Tabor surface is now available from MMM, vapor deposited gold on aluminum or H-film, which looks like a good prospect to be evaluated.

4.3 THERMAL MATERIALS

Thermal control materials have been examined with regard to the anticipated boost, trajectory and encounter environment to determine the effects on both optical and physical properties. Possible materials include the following table:

Material	Temperature (°F)	Utilization
Aluminum foil (0.00025 - 0.001) Tissue Paper (0.002 - 0.005) Quartz Paper (0.002 - 0.005) Fiberglass (0.002 - 0.005) Aluminized mylar (0.002 - 0.005)	-320 to +250	Super Insulation
Polished aluminum	0 to 120	Temperature Control Surface
Stainless Steel	-320 to +250	Insulation Containment
Aluminum Foil (0.006 - 0.010)	-200 to +150	Shutter
Freon 11, 12, 21, 114	0 to 120	Actuation Fluid
Aluminum - Beryllium	0 to 120	Bellows Actuator
Invar - Manganese	0 to 120	Bimetallic Actuator
Alodine on aluminum	0 to 120	Temperature Control Surface
Dow 10/17 on magnesium	0 to 120	Temperature Control Surface
Anodized aluminum	0 to 120	Temperature Control Surface

There is no evidence of a problem in any of the thermal materials in the specified space environment. The aluminum foil shutter will be perforated or roughened by 300 small micrometeorids/cm^2 in a year's time. This is not believed to be a problem, but justifies experimental checking in the laboratory.

The internal nuclear radiation dose on the Freons will produce very slight degradation. As long as the refrigeration lines and coils are made of metals resistant to chloride corrosion (this means no aluminum), there will be no problem with the Freon.

SECTION 5
INSULATION INVESTIGATION

5.1 MULTIPLE-FOIL INSULATION

Preliminary investigations of possible Comet Probe designs Figures 2-5 and 2-6 indicate a highly efficient, low-weight insulation to be used to prevent compartment heating from direct and/or reflected solar energy when the spacecraft is at 1 A.U. This same insulation must also contain the compartment heat generation to maintain temperature control as the spacecraft travels away from the sun. Multiple-foil, or super-, insulation is considered strongly for application as the heat shield material due to its relatively high resistance to heat flow and low density. Preliminary calculations require an over-all insulation effective emissivity of 0.01 or less to reduce the heat leakage to an acceptable level. The term effective emissivity, ϵ_{eff}, is derived from

$$\epsilon_{eff} = \frac{(Q/A)\ Leak}{\sigma(T_o^4 - T_c^4)} \qquad (5\text{-}1)$$

where

(Q/A) Leak = allowable heat leak either into, or out of, equipment compartment $\left(\frac{Btu}{hr\ ft^2}\right)$

T_o = outside surface temperature (^oR)

T_c = inside or compartment temperature (^oR)

For optimum insulation performance, radiation is the major mode of heat transfer through the multiple foils. Therefore, the performance criteria affecting the radiation heat balances equation is more desirable than the norally used apparent conductivity parameter in the Fourier equation. The factor should be the effective emissivity since this permits the more logical correlation and utilization

5.1.1 Insulation Attachment

Considerable data has been published on pure superinsulation performance and these results indicate feasibility in the insulation design. See Table 5-1. However, little data or practical experience has been reported on the problem of thermal shorting due to insultation discontinuities, penetrations and edge effects. Therefore, Philco has constructed an insulation test apparatus and has begun to evaluate numerous techniques for mounting multiple-foil insulation. These tests will establish optimum methods of application for generalize problem areas such as joints, corners, penetrations, edges and support techniques.

Promising materials will be initially screened in the pure insulation performance rig and the most efficient will then undergo further testing. These tests will include support and joint evaluations as illustrated in Figure 5-1, and attachment configurations as shown in Figure 5-2. The results of these tests will be used to develop an insulation heat shield which will undergo individual testing. A typical proposed heat shield is shown in Figure 5-3.

Table 5-1 Insulation Properties in Deep Vacuum

INSULATION	SOURCE	NO. OF LAYERS	THICKNESS (in)	DENSITY (lbs/ft^3)	TEMPERATURE GRADIENT (^oF)	ϵ_{eff}
Powder Type						
Perlite (-80 mesh)	[Fulk et al, 1956]	---	1.0	8.7	-320 to + 80	0.021
Silica aerogel with aluminum powder		---	1.0	6.0	-320 to + 80	0.012
Fiber Type						
Fiberglass (Type A)	[Verschoor and Greebler, 1952]	---	1.0	4.63	+ 90 to +210	0.010
Glass Fiber - heated felt (AA fiber)	[Christiansen and Hollingsworth, 1958]	---	1.0	8.0	-320 to + 75	0.014
Multiple Layer Type						
Linde SI-4	[Riede and Wang, 1960]	60	1.0	4.7	-320 to + 70	0.00089
NRC - 2 - aluminized mylar	[NRC, 1959]	60	1.0	2.2	-423 to + 80	0.0022
0.008 in. glass paper 0.00023 in. aluminum foil	[Kropschot, Schrodt and Hunter, 1960]	55	1.0	7.5	-320 to + 80	0.0012
WDL results aluminized mylar	----	60	1.0	1.44	-320 to + 70	0.0031
	----	60	0.75	1.92	-320 to + 61	0.0033
	----	60	0.50	2.88	-320 to + 59	0.0071
General Electric	[Casagrande, 1962]	30	0.50	1.43	-320 to + 67	0.011
1/4 mil aluminized mylar		60	0.50	2.68	-320 to + 76	0.0045

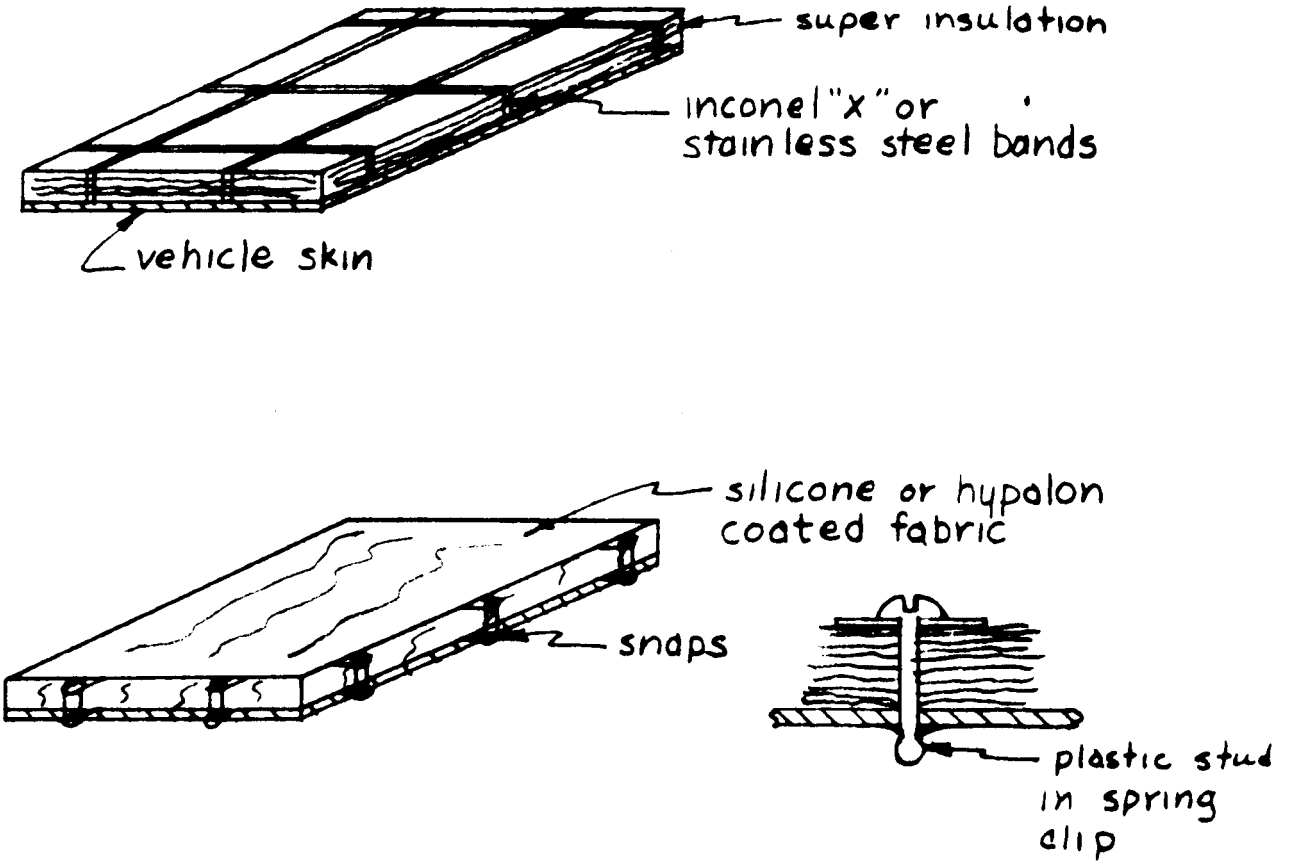

Fig. 5-1 Possible Support or Attachment Methods

(a) BUTT JOINT

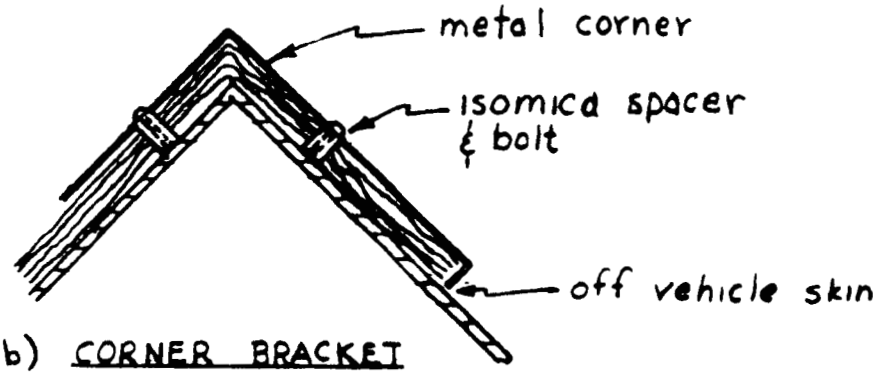

(b) CORNER BRACKET

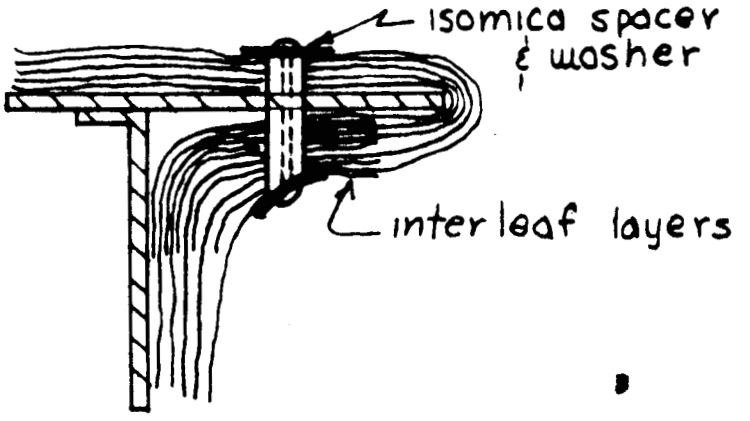

(c) OVERLAPPED CORNER JOINT

Fig. 5-2 Possible Joint Mehtods

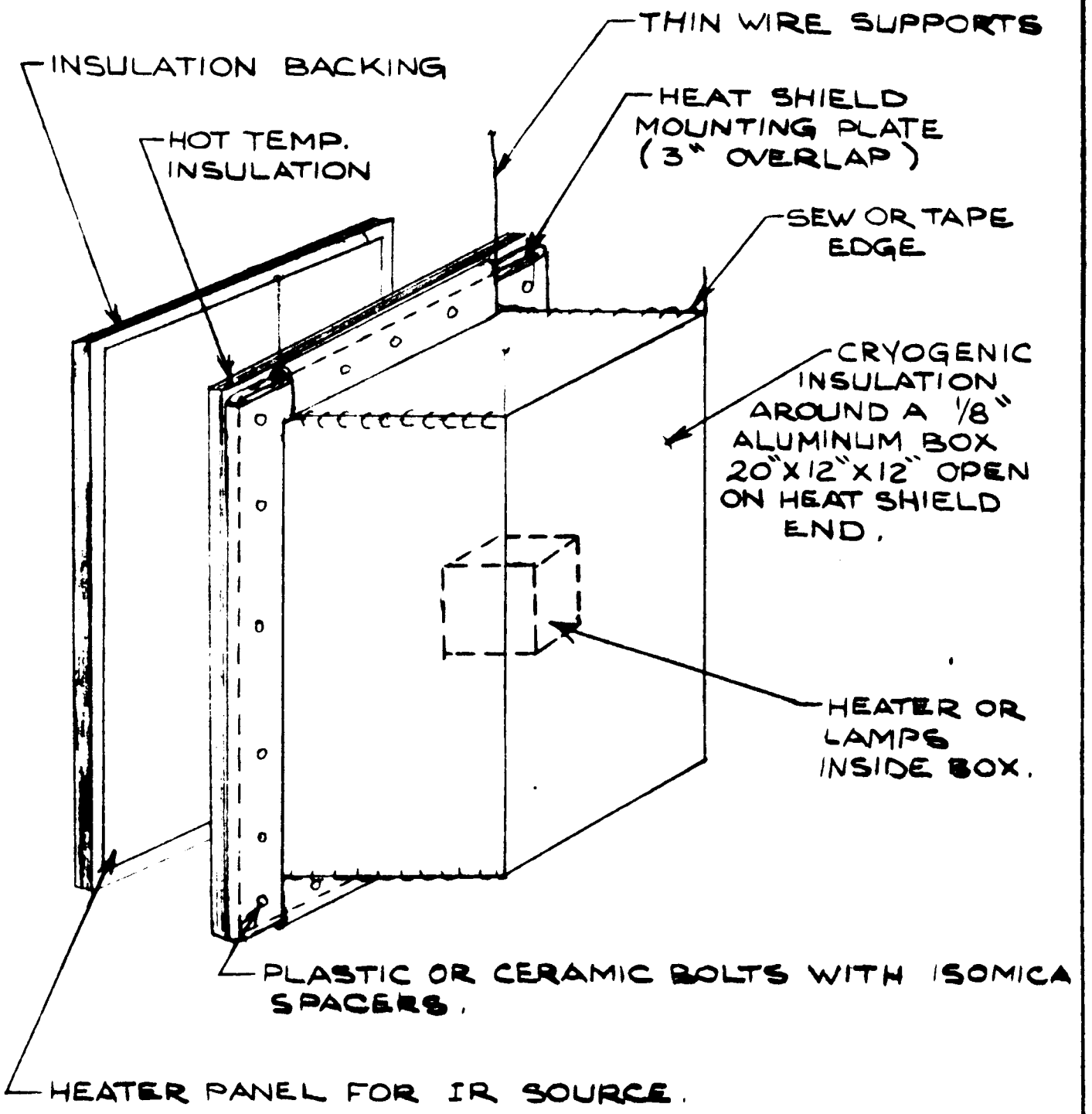

Fig. 5-3 Possible Heat Shield Rig

SECTION 6
RECOMMENDATIONS

6.1 RECOMMENDATIONS

Although a major portion of the Mariner-C thermal design and technology is directly applicable to the Comet Probe design, particularly in the active temperature control areas, there are three critical areas that require additional study. One is a study of methods of mounting multiple-foil insulation with minimum thermal shorting that will withstand the acceleration and vibration environment imposed during boost. A brief description of a test program being conducted by Philco has been included in this report. However, much more inclusive investigation, one that combines analysis with experimental data, is required.

Another study, as indicated in the coatings portion of this report, is the testing of certain coatings for the total amount of equivalent sun hours (E.S.H.) that will occur in a Comet Probe mission. Most coatings have undergone exposures of the order of 600 to 1000 E.S.H. while the requirement for a Comet Probe is a factor of 4 to 5 greater.

The final recommended study is an evaluation of possible methods of obtaining a structural joint that would change its thermal characteristics after launch. Of particular interest is the use of isotope-impregnated materials which can change their properties at some predetermined point in the trajectory.

SECTION 7

REFERENCES

AFML, Space Materials Handbook, Air Force Materials Laboratory, ML-TDR-64-40; March, 1964.

Betz, Howard, O. Harry Olson, Bert D. Schurin and James C. Morris, "Determination of Emissivityand Reflectivity Data on Aircraft Structural Materials", Part II, ASTIA-AD202493; October, 1958.

Casagrande, R. D., "Test Results of Measurements of Thermal Conductivities of 1/4 Mil Aluminized Mylar Superinsulation", General Electric M.S.D. IR 4142-308; May, 1962.

Christiansen, R. M. and M. Hollingworth, Jr., "The Performance of Glass Fiber Insulations Under High Vacuum", Proceedings of the 1953 Cryogenics Engineering Conference; pp. 141-153; 1958.

Fulk, M. M., et al, "Progress Report on Powder Insulations", Laboratory Note 56-7, N.B.S. Cryogenics Engineering Lab., Boulder, Colorado; July, 1956.

Hultquist, A. E. and M. E. Sibert, "Preparation of Temperature Control Surfaces by Anodization of Aluminum", Part II, Electrochemical Technology, 2, No. 1-2; February, 1964.

Kropschot, R. H., Schrodt, J. E., and B. J. Hunter, "Multiple-Lazer Insulation", Advances in Cryogenic Engineering, Vol. 5, Plenum Press, New York; 1960.

LMSC Process Bulletin 55.

Lehr, S. N., L. J. Martire and V. J. Tronolone, "Equipment Design Considerations for Space Environment", STL/TR-990-6032, RU000; February, 1962.

MMM Data Sheet Y.

National Research Corporation (NRC).

Philco, Solar Probe Study, Book B. Appendix 3, Thermal, WDL-TR2133; August, 1963.

Riede, P. M. and Wang, DI-J., "Characteristics and Applications of Some Superinsulations", Advances in Cryogenic Engineering, Vol. 5, Plenum Press, New York; 1960.

Shipley, W. S. and T. O. Thostesen, "Radiative Properties of Surfaces Considered for Use on the Explorer Satellites and Pioneer Space Probes", JPL-Memorandum 20-194.

Sibert, M. E., "Inorganic Surface Coatings for Space Applications", LMSC 3-77-61-12; August, 1961.

Streed, E. R. and E. M. Beveridge, "The Study of Low Solar Absorptance Coatings for a Solar Probe Mission", Symposium on Thermal Radiation of Solids, San Francisco; March, 1964.

Verschoor, V. D. and P. Greebler, "Heat Transfer by Gas Conduction and Radiation in Fibrous Insulation", Torous, ASME; (August, 1952. ,

Wood, W. D., H. W. Deem and C. F. Lucks, "Thermal Radiative Properties of Selected Materials", Defense Metals Information Center, DMI-177, Vol. 1 and 2; November, 1962.

Zerlaut, G. A. and Y. Harada, "Stable White Coatings", Jet Propulsion Laboratory-ARF Project, ARF 3207-14; 1963a.

Zerlaut, G. A. and Y. Harada, "Stable White Coatings", Jet Propulsion Laboratory-IITRI Project, IITRI-C207-25; July, 1963b.

Zerlaut, G. A. and Y. Harada, "Stable White Coatings", Jet Propulsion Laboratory-IITRI Project, IITRI-C207-27; November, 1963c.

HEAT BALANCE - ISOTOPIC SUPPLY

A.1 SYSTEM SCHEMATIC

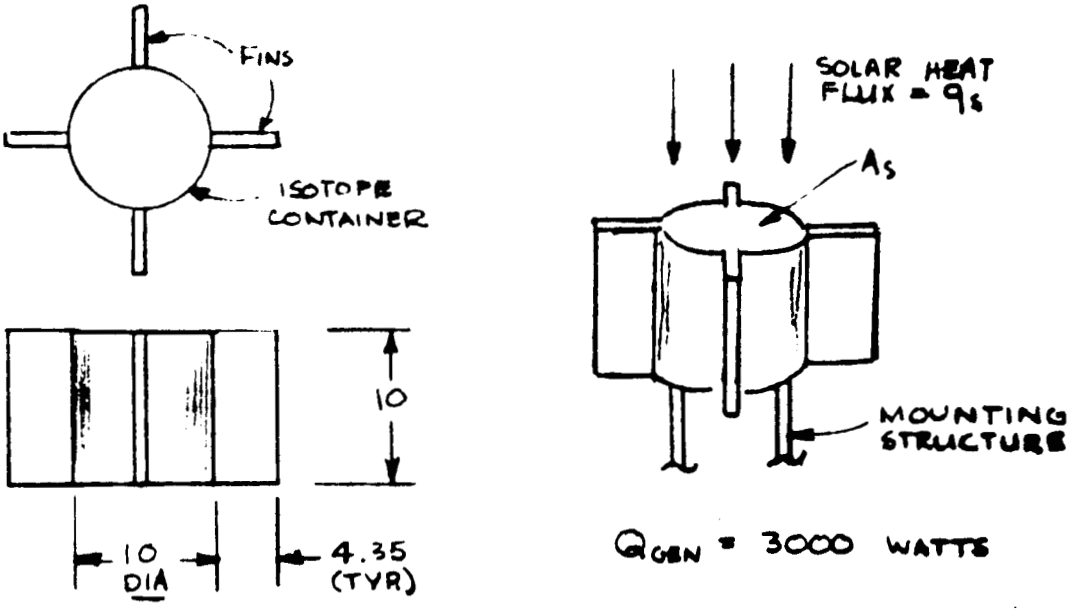

A.2 ASSUMPTIONS

To simplify the calculation, the following assumptions are made:

a. Conduction through the support structure is neglected.

b. A uniform surface temperature is assumed.

c. Heat transfer from the face away from the sun (i.e., the face that "sees" any other part of itself or the vehicle.

d. The entire outer surface is assumed to radiate to space @ $0^{\circ}R$, and this surface (including fins) is assumed not to "see" any other part of itself or the vehicle.

e. The surface absorptivity is assumed = 1.

A.3 ANALYSIS

A simple heat balance yields:

$$(1) \quad q\ A_t = Q_{gen} + q_s\ A_s\ \alpha_s = \sigma \mathcal{F} (T^4 - T\infty^4) A_t$$

where

Q_{gen} = isotope heat generation

q_s = incident solar heat flux

A_s = area exposed to solar heat flux

q = heat loss from surface

T = surface temperature

σ = 0.1714×10^{-8} Btu/hr.ft^2 $^oR^4$

$T\infty$ = 0 ^oR

$\mathcal{F}$ = ϵ

ϵ = surface emissivity

α_s = surface absorptivity (assume = 1.0)

Since the size of system has been established, eq. (1) will be solved for T as function of ϵ and q_s, where q_s = f(A.U.).

A.4 CALCULATION

$$A_s = \frac{\pi(5)^2}{144} = 0.545\ Ft^2$$

$$A_t = 0.545 + \frac{\pi(10)(10)}{144} + \frac{(4.35)(10)(8)}{144} = 5.145\ Ft^2$$

$$Q_{gen} = (3000)(3.413) = 10250\ Btu/hr.$$

Incorporating these values in (1):

$$10250 + 0.545\ q_s = (0.1714)(5.145)\left(\frac{T}{100}\right)^4 \epsilon$$

$$(2) \quad \left(\frac{T}{100}\right)^4 = \frac{10250 + 0.545\ q_s}{0.88\ \epsilon}$$

Eq. (2) will be solved for T.

1 A.U.

At 1 A.U., $q_s = 442$ Btu/hr.Ft^2 and

$$\left(\frac{T}{100}\right)^4 = \frac{10250 + (0.545)(442)}{0.88\epsilon} = \frac{10491}{0.88\epsilon}$$

ϵ	T($^\circ$F)
0.2	1104
0.4	854
0.6	728
0.8	645
1.0	585

2 A.U.

At 2 A.U., $q_s = 110$ Btu/hr.Ft^2 and

$$\left(\frac{T}{100}\right)^4 = \frac{10250 + (0.545)(110)}{0.88\epsilon} = \frac{10310}{0.88\epsilon}$$

ϵ	T($^\circ$F)
0.2	1095
0.4	848
0.6	722
0.8	640
1.0	582

These results are plotted in Figure 8.10.

Effect of Interchange Factor

The previous calculations assume $\mathcal{F} = 1$, i.e., $\bar{F}$ in the expression

$$(3) \quad \mathcal{F}_{12} = \frac{1}{\frac{1}{F_{12}} + \left(\frac{1}{\epsilon_1} - 1\right) + \frac{A_1}{A_2}\left(\frac{1}{\epsilon_2} - 1\right)}$$

where $A_2 = \infty$. To properly bound this calculation (since F_{12} will, in fact be some what less than unity), we will assume $F_{12} = 0.7$ and repeat the calculation for 1 A.U. (F_{12} will probably be between 0.7 and 1.0, but the intent here is to bound the problem).

$$(4) \quad \mathcal{F}_{12} = \frac{1}{\frac{1}{0.7} + \left(\frac{1}{\epsilon_1} - 1\right)} = \frac{1}{0.43 + \frac{1}{\epsilon}} = \frac{1}{1 + 0.43\epsilon}$$

Eq. (2) now becomes (for 1 A.U.):

$$\left(\frac{T}{100}\right)^4 = \frac{10491}{0.88}\left(\frac{1 + 0.43\epsilon}{\epsilon}\right) = 11920\left(\frac{1 + 0.43}{\epsilon}\right)$$

ϵ	T(°F)
0.2	
0.4	907
0.6	794
0.8	730
1.0	683

The effect of the interchange factor is illustrated in Figure 8-10 and is relatively insignificant with regard to thermo-electri characteristics of the isotope.

B.1 SYSTEM SCHEMATIC

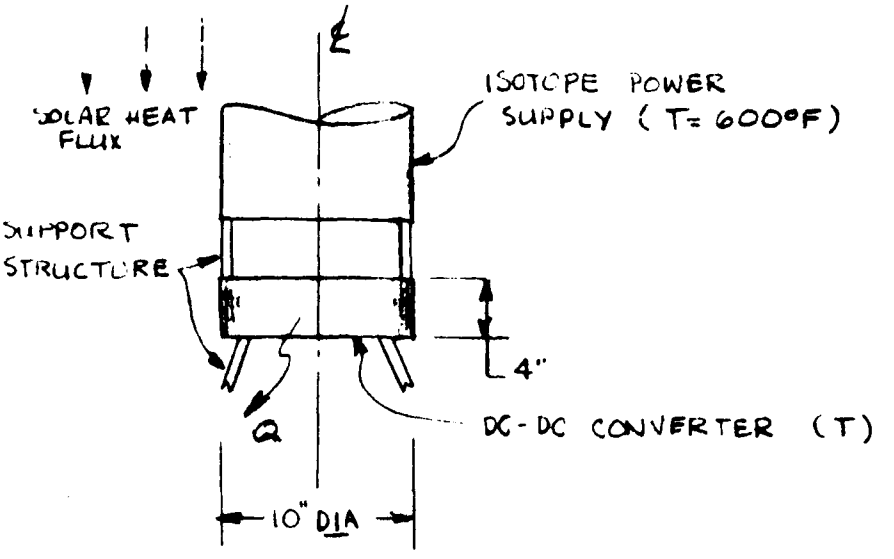

Q_{max} = 30 WATTS. This value may vary from 3 to 30.

T < 150°F

B.2 ASSUMPTIONS

To simplify the calculation, the following assumptions are made:

a. The simplified geometry of Figure 2 is assumed to apply.

b. Conduction through the support structure is neglected.

c. Uniform surface temperatures are assumed throughout.

d. The remainder of the vehicle is assumed to be a flat plate at 70°F, and not "seen by the sides of the converter.

e. The sides are assumed to "see" only space at 0°R; and the end facing the isotope only the power supply.

f. Reflections and re-radiation are neglected.

g. All surface emissivities are assumed the same.

B. 3 ANALYSIS

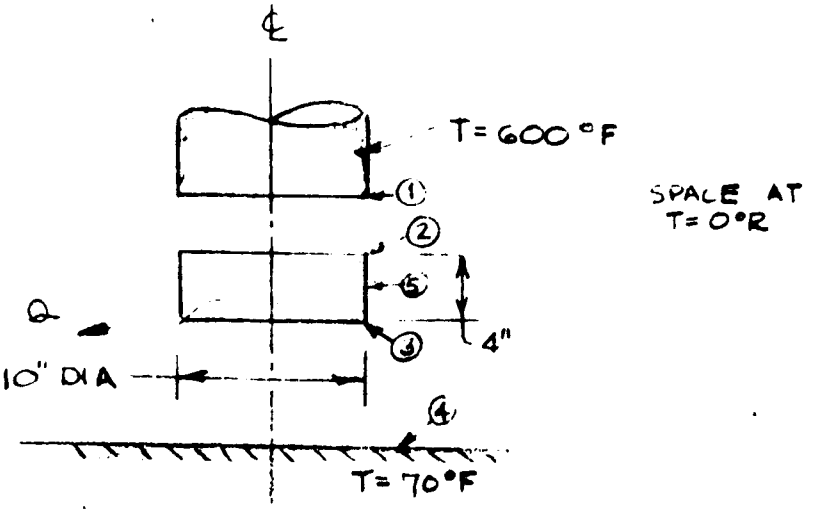

A heat balance on the DC-DC converter is approximated by

$$q_{12} + Q = q_{34} + q_{50} \qquad \text{(B-1)}$$

for steady state. Then,

$$\sigma \mathcal{F}_{12}\, A_1 (T_1^4 - T_2^4) + Q = \sigma \mathcal{F}_{34}\, A_3 (T_3^4 - T_4^4) + \sigma \mathcal{F}_{50}\, A_5 (T_5^4 - T_o^4) \qquad \text{(B-2)}$$

From the geometry and our assumptions:

$$A_1 = A_3 = A$$

$$T_2 = T_3 = T_5 = T$$

$$T_o = 0\ ^\circ R$$

and (B-2) becomes

$$\sigma \mathcal{F}_{12}\, A (T_1^4 - T^4) + Q = \sigma \mathcal{F}_{34}\, A (T^4 - T_4^4) + \sigma \mathcal{F}_{50}\, A_5\, T_5^4$$

$$(\sigma \mathcal{F}_{34}\, A + \sigma \mathcal{F}_{12}\, A + \sigma \mathcal{F}_{50}\, A_5)\, T^4 = \sigma \mathcal{F}_{12}\, A\, T_1^4 + \sigma \mathcal{F}_{34}\, A\, T_4^4 + Q$$

$$T^4 = \frac{\sigma A (\mathcal{F}_{12}\, T_1^4 + \mathcal{F}_{34}\, T_4^4) + Q}{\sigma A (\mathcal{F}_{12} + \mathcal{F}_{34}) + \sigma A_5 \mathcal{F}_{50}} \qquad \text{(B-3)}$$

The factors $\mathcal{F}_{50}$, $\mathcal{F}_{12}$, and $\mathcal{F}_{34}$ are evaluated below based on eq. (4)

$\underline{\mathcal{F}_{50}}$

For a surface radiating directly and only to space,

$$\mathcal{F}_{50} = \epsilon_5 = \epsilon \qquad \text{(B-6)}$$

$\underline{\mathcal{F}_{12}}$

Treat as two discs. Assume no effect from space (either losses to or radiation from the surroundings.

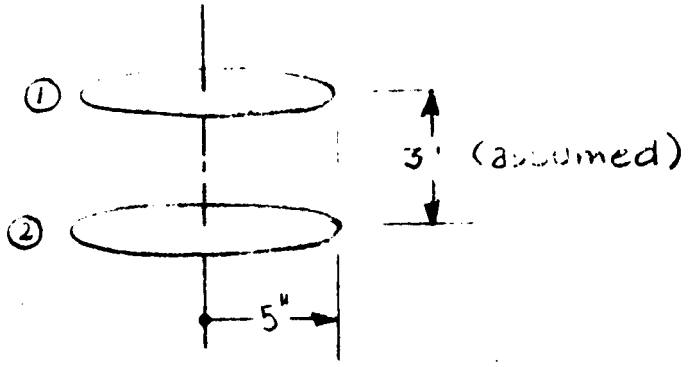

For the above configuration:

$\mathcal{F}_{12} \sim 0.5$

$$\therefore \mathcal{F}_{12} = \frac{1}{\frac{1}{0.5} + \left(\frac{1}{\epsilon_1} - 1\right) + \frac{A_1}{A_2}\left(\frac{1}{\epsilon_2} - 1\right)} \qquad \epsilon_1 = \epsilon_2 = \epsilon, \quad A_1 = A_2$$

$$= \frac{1}{2 + \left(\frac{1}{\epsilon} - 1\right) + \left(\frac{1}{\epsilon} - 1\right)} = \frac{\epsilon}{2\epsilon + 2 - 2\epsilon}$$

$$= \frac{\epsilon}{2} \qquad \text{(B-7)}$$

$\mathcal{F}_{34}$

Treat as two discs. One much larger than the other. (The larger disc is an approximation of the effect of the heat shield and the antenna).

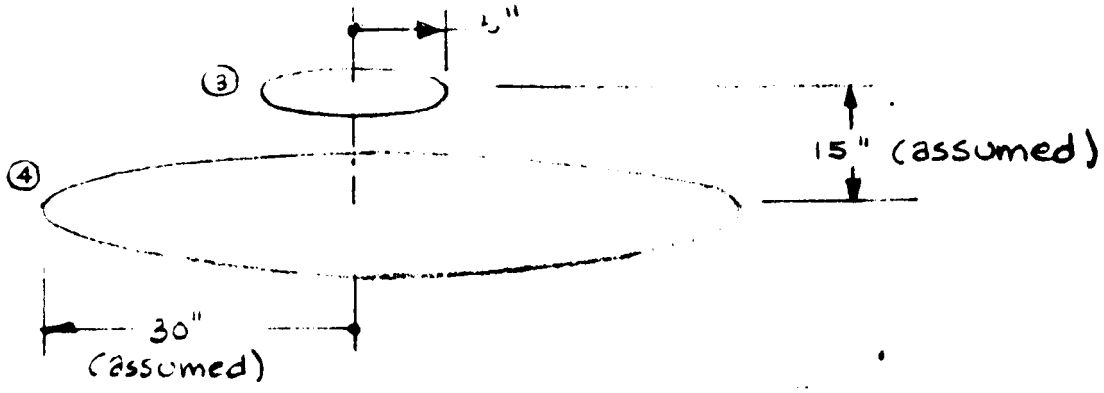

For the given configuration:

$\mathcal{F}_{34} \sim 0.8$

$$\therefore \mathcal{F}_{34} = \frac{1}{\frac{1}{0.8} + \left(\frac{1}{\epsilon_3} - 1\right) + \frac{A_3}{A_4}\left(\frac{1}{\epsilon_4} - 1\right)} \qquad \epsilon_3 = \epsilon_4 = \epsilon, \quad A_3 \ll A_4$$

$$= \frac{\epsilon}{1.25\epsilon + (1 - \epsilon)}$$

$$= \frac{4\epsilon}{4 + \epsilon} \qquad \text{(B-8)}$$

B.5 CALCULATION

Combining (B-6), (B-7), and (B-8) with (B-5):

$$\left(\frac{T}{100}\right)^4 = \frac{0.0936\left[12600(\epsilon/2) + 790\left(\frac{4\epsilon}{4+\epsilon}\right)\right] + Q}{0.0936\left(\frac{\epsilon}{2} + \frac{4\epsilon}{4+\epsilon}\right) + 0.1495\epsilon}$$

$$= \frac{590\epsilon + 296\left(\frac{\epsilon}{4+\epsilon}\right) + Q}{0.1963\epsilon + 0.374\left(\frac{\epsilon}{4+\epsilon}\right)} \qquad \text{(B-9)}$$

(B-9) can be solved for various vales of ϵ and Q.

$\epsilon = 0.2$

$$\left(\frac{T}{100}\right)^4 = \frac{(590)(0.2) + (296)\left(\frac{0.2}{4.2}\right) + Q}{(0.1963)(0.2) + 0.374\left(\frac{0.2}{4.2}\right)}$$

$$= \frac{132.1 + Q}{0.0571} \qquad \text{(B-10)}$$

Q (Watts)	Q (Btu/Hr.)	T ($^\circ$R)	T ($^\circ$F)
0	0	694	234
5	17.1	715	255
10	34.1	734	274
15	51.2	753	293
20	68.2	769	309
25	85.3	786	326
30	102.5	801	341

$\varepsilon = 0.9$

$$\left(\frac{T}{100}\right)^4 = \frac{(590)(0.9) + (296)\left(\frac{0.9}{4.9}\right) + Q}{(0.1963)(0.9) + (0.374)\left(\frac{0.9}{4.9}\right)}$$

$$= \frac{585.4 + Q}{0.2458} \qquad \text{(B-11)}$$

Q (Watts)	Q (Btu/Hr.)	T (^{o}R)	T (^{o}F)
0	0	699	239
5	17.1	704	244
10	34.1	708.5	248.5
15	51.2	713	253
20	68.2	718	258
25	85.3	723	263
30	102.5	727	267

B.6 ADDITION OF FINS

The temperature levels computed in Section B.5 are in excess of the allowable value (150°F, max.) for the DC-DC converter. One way to alleviate this problem, fins could be added to the outer surface. Assuming fins similar to those proposed for the isotope power supply, we obtain a configuration as shown in the adjacent sketch. Assuming that $\mathcal{F}_{50} = \epsilon$ (i.e., that all surfaces radiated directly to space). Thus, in eq. (5) only A_5 will be modified with approximations made above. For this case, A_5 becomes:

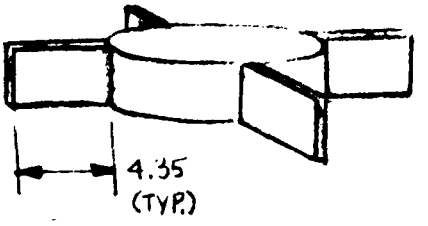

$$A_5 = 0.373 + \frac{(4.35)(4)}{144}(8) = 1.840 \text{ Ft}^2$$

(B-9) becomes:

$$\left(\frac{T}{100}\right)^4 = \frac{590\epsilon + 296\left(\frac{\epsilon}{4+\epsilon}\right) + Q}{0.3618\epsilon + 0.374\left(\frac{\epsilon}{4+\epsilon}\right)} \qquad \text{(B-12)}$$

$\epsilon = 0.2$

$$\left(\frac{T}{100}\right)^4 = \frac{132.1 + Q}{0.0901} \qquad \text{(B-13)}$$

Q (Watts)	Q (Btu/Hr.)	T (°R)	T (°F)
0	0	619	159
5	17.1	638	178
10	34.1	655	195
15	51.2	672	212
20	68.2	687	227
25	85.3	701	241
30	102.5	714	254

$\epsilon = 0.9$

$$\left(\frac{T}{100}\right)^4 = \frac{585.1 + Q}{(0.3618)(0.9) + (0.374)\left(\frac{0.9}{4.9}\right)}$$

$$= \frac{585.1 + Q}{0.3938} \qquad \text{(B-14)}$$

Q		T	
(Watts)	(Btu/Hr.)	(^{o}R)	(^{o}F)
0	0	621	161
5	17.1	627	167
10	34.1	630	170
15	51.2	634	174
20	68.2	638	178
25	85.3	643	183
30	102.5	646	186